Supporting Information

Accessing unsymmetrical Ru(II) bipyridine complexes: a versatile synthetic mechanism for fine tuning photophysical properties.

Lukas Hallen,[a] Alexander M. Horan,[b] Brendan Twamley,[a] Eoghan M. McGarrigle,*[b] Sylvia M. Draper*[a,c]

Email: smdraper@tcd.ie, eoghan.mcgarrigle@ucd.ie

[a] School of Chemistry, Trinity College Dublin, the University of Dublin, Dublin 2, Ireland

[b] SSPC, the SFI Research Centre for Pharmaceuticals, Centre for Synthesis & Chemical Biology, UCD School of Chemistry, University College Dublin, Belfield, Dublin 4, Ireland

[c] AMBER (Advanced Materials and Bioengineering Research) Centre, Trinity College Dublin, Dublin 2, Ireland

Contents

1.0 Experimental Information and Equipment

^{1}H NMR, ^{13}C{^{1}H} NMR, ^{31}P NMR, and ^{19}F NMR spectra were recorded using a Bruker Advance DPX-400 MHz, Bruker AV-400 MHz, or Bruker AV-600 MHz spectrometer in $CDCl_3$ or CD_3CN with tetramethylsilane as the internal standard. Electrospray ionization (ESI) mass spectra were recorded on a micromass LCT electrospray mass spectrometer, or a Bruker MicrOTOF-Q-III mass spectrometer. Atmospheric Pressure Chemical Ionization (APCI) mass spectra were recorded on a Bruker MicrOTOF-Q-III mass spectrometer. Accurate MS were referenced against leucine enkephalin (555.6 g mol-1) or [Glu1]-Fibrinopeptide B (1570.6 g mol-1) and were reported within 5 ppm. MALDI-TOF mass spectra were recorded on a Waters MALDI-QTOF Premier spectrometer using an α-cyano-4-hydroxy cinnamic acid matrix.

UV-vis absorption spectra were recorded on a Shimadzu UV-2450 spectrophotometer. Emission and excitation spectra, and emission quantum yields were recorded on a Horiba FluoroMax-4 spectrofluorometer.

Emission quantum yields of solutions were measured using the single-point relative method, using Fluorescein in 0.1 M aq. NaOH (for **L1**, **L2** and **L3**) or $[Ru(bpy)_3](PF_6)$ in MeCN (for **Ru1, Ru2** and **Ru3**) as the reference, at RT.[1,2] $[Ru(bpy)_3](PF_6)_2$ was purchased from TCI Europe n.v. and used without purification. Fluorescein was purchased from Fluka and used without purification. Emission lifetime measurements were performed on a Horiba-Jobin-Yvon FluoroLog FL-3-11 spectrofluorometer with a TBX-04-D picosecond photodetection module using a NanoLED pulsed diode laser excitation source (λ_{ex} = 460 nm for **Ru1**, **Ru2** and **Ru3**).

2.0 Ligand Synthesis

N,*N*-Diphenyl-4-(4,4,5,5-tetramethyl-1,3,2-dioxaborolan-2-yl)aniline and 4-(*N*,*N*-diphenylamino)phenylacetylene were prepared according to literature procedures.[3 4]

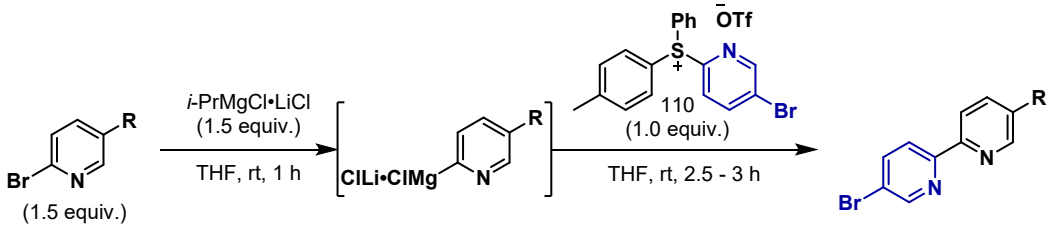

Scheme S1. Synthesis of bis-heteroaryls using Grignard reagents and sulfonium salts

Bromopyridine (1.5 equiv.) was added to an oven-dried crimp top vial which was sealed, evacuated and purged with N_2 three times. Bromopyridine was dissolved in dry THF (0.3 M) at rt. *i*-PrMgCl•LiCl (1.5 equiv., 1.2 M in THF) was added dropwise to the stirring solution over 2 min. The reaction was allowed to stir at rt for 1 h. Sulfonium salt (1.0 equiv.) was added to a separate oven-dried crimp top vial which was sealed, evacuated and purged with N_2 three times. Sulfonium salt was dissolved in dry THF (0.3 M) and added dropwise down the side of the vial to the Grignard reagent solution over 2 min. The reaction was allowed to stir at rt for the time

stated. Saturated aq. NH_4Cl (5 mL) was added slowly to quench any excess Grignard reagent. The product was extracted with EtOAc (3 x 10 mL), the combined organic layers were washed with H_2O (20 mL) and brine (20 mL) and dried over anhydrous Na_2SO_4. Following concentration *in vacuo*, the desired product was isolated by FCC.

2-Bromo-5-(4-(trifluoromethyl)phenyl)pyridine (P1)

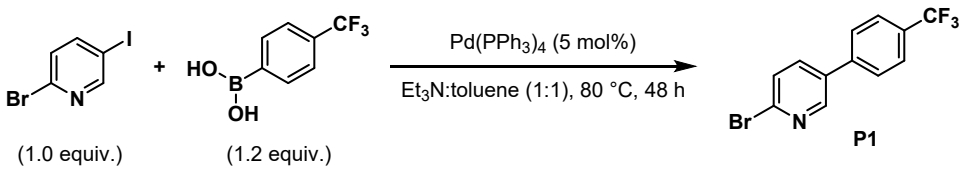

2-Bromo-5-iodopyridine (1.14 g, 4.00 mmol), 4-(trifluoromethyl)phenylboronic acid (0.91 g, 4.8 mmol) and $Pd(PPh_3)_4$ (0.145 g, 0.200 mmol) were added to an oven-dried crimp top vial, which was evacuated and purged with N_2 three times. Dry Et_3N (4 mL) and dry toluene (4 mL) were added to the vial and the reaction mixture was heated to 80 °C for 48 h, then concentrated *in vacuo*. Purification by FCC (5% Et_2O in pentane) gave product **P1** as a white solid (0.478 g, 39%).

^{1}H NMR (500 MHz, Chloroform-*d*) δ 8.60 (d, *J* = 2.5 Hz, 1H,), 7.77 – 7.72 (m, 3H,), 7.66 (d, *J* = 8.2 Hz, 2H), 7.59 (d, *J* = 8.3 Hz, 1H).

^{13}C NMR (126 MHz, Chloroform-*d*) δ 148.7 (CH), 142.1 (CBr), 140.2 (C_q), 137.1 (CH), 134.8 (C_q), 130.8 (q, *J* = 32.8 Hz, C_q), 128.4 (CH), 127.5 (CH), 126.4 (q, *J* = 3.8 Hz, CH), 124.1 (q, *J* = 272.2 Hz, CF_3).

^{19}F NMR (470 MHz, Chloroform-*d*) δ -62.7 (CF_3).

HRMS (ESI-TOF) *m/z*: $[M+H]^+$ Calc'd for: $C_{12}H_7BrF_3N$ 301.9787, 303.9767; found: 301.9788, 303.9768.

5-Bromo-5'-(4-(trifluoromethyl)phenyl)-2,2'-bipyridine (4a)

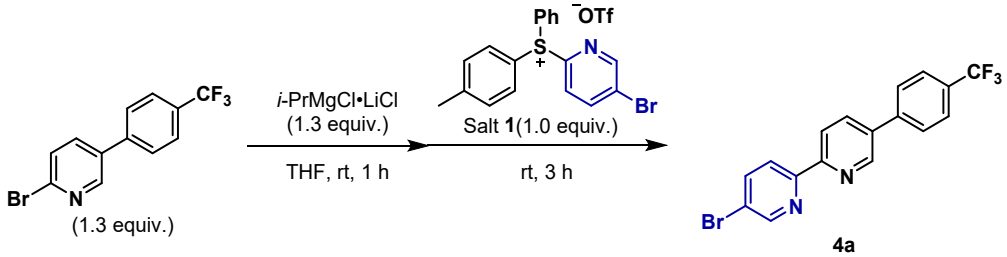

Product **4a** was synthesised *via* general procedure A using **P1** (0.30 g, 0.99 mmol) and bromopyridyl sulfonium salt **1** (0.385 g, 0.760 mmol). Salt **1** was synthesised according to previously published literature procedures.[5] The Grignard reagent was formed at rt for 1 h and the ligand coupling reaction was stirred at rt for 3 h. Purification by FCC (10% Et_2O in pentane) gave bipyridine **4a** as a white solid (114.1 mg, 40%).

TLC R_f = 0.36 (10% Et_2O in pentane).

^{1}H NMR (400 MHz, Chloroform-*d*) δ 8.90 (d, *J* = 2.3 Hz, 1H), 8.74 (d, *J* = 2.3 Hz, 1H), 8.48 (d, *J* = 8.2 Hz, 1H), 8.36 (d, *J* = 8.4 Hz, 1H), 8.02 (dd, *J* = 8.2, 2.3 Hz, 1H), 7.96 (dd, *J* = 8.4, 2.3 Hz, 1H), 7.75 (s, 4H).

^{13}C NMR (101 MHz, Chloroform-*d*) δ 155.0 (C_q), 154.2 (C_q), 150.5 (C_q), 147.9 (C_q), 141.2 (C_q), 139.7 (CH), 135.6 (CH), 135.5 (C_q), 130.5 (q, *J* = 32.5 Hz, C_q), 127.5 (CH), 126.3 (q, *J* = 3.8 Hz, CH), 124.2 (q, *J* = 272.2 Hz, CF_3), 122.5 (CH), 121.5 (CBr), 121.2 (CH).

^{19}F NMR (376 MHz, Chloroform-*d*) δ -62.6 (CF_3).

HRMS (ESI-TOF) *m/z*: $[M+H]^+$ Calc'd for: $C_{17}H_{11}BrF_3N_2$ 379.0052, 381.0033; found: 379.0053, 381.0033.

***N*,*N*-Diphenyl-4-(5'-(4-(trifluoromethyl)phenyl)-[2,2'-bipyridin]-5-yl)aniline (L1ac)**

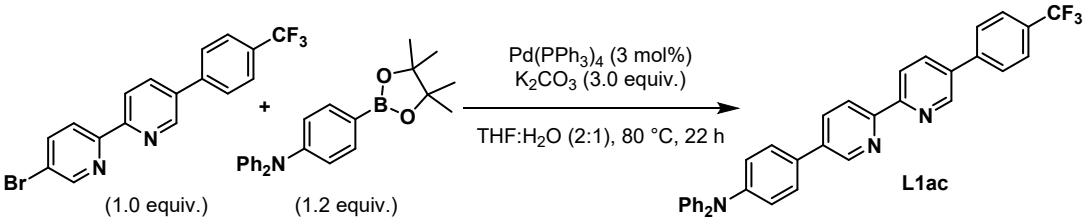

Bipyridine **4a** (69 mg, 0.18 mmol), *N*,*N*-diphenyl-4-(4,4,5,5-tetramethyl-1,3,2-dioxaborolan-2-yl)aniline (82 mg, 0.22 mmol), K_2CO_3 (75 mg, 0.54 mmol) and $Pd(PPh_3)_4$ (5.8 mg, 0.0033 mmol) were added to an oven-dried crimp top vial, which was evacuated and purged with N_2 three times. THF (0.6 mL) and H_2O (0.3 mL) were added to the vial and the reaction mixture was heated to 80 °C for 22 h. The reaction mixture was then cooled to rt, diluted with H_2O (20 mL) and extracted with CH_2Cl_2 (3 x 20 mL). The combined organic layers were dried over anhydrous Na_2SO_4. Purification by FCC (20% Et_2O in pentane) gave product **L1ac** as a yellow solid (86.5 mg, 88%).

TLC R_f = 0.14 (20% Et_2O in pentane).

^{1}H NMR (500 MHz, Chloroform-*d*) δ 8.96 – 8.91 (m, 2H), 8.54 (d, *J* = 8.3 Hz, 1H), 8.50 (d, *J* = 8.2 Hz, 1H), 8.05 (dd, *J* = 8.3, 2.4 Hz, 1H), 8.02 (dd, *J* = 8.2, 2.4 Hz, 1H), 7.77 (s, 4H), 7.55 (d, *J* = 8.7 Hz, 2H), 7.33 – 7.27 (m, 4H), 7.20 – 7.14 (m, 6H), 7.10 – 7.05 (m, 2H).

^{13}C NMR (126 MHz, Chloroform-*d*) δ 155.8 (C_q), 153.9 (C_q), 148.4 (C_q), 147.9 (CH), 147.5 (C_q), 147.4 (CH), 141.4 (C_q), 136.4 (C), 135.5 (CH), 135.0 (C_q), 134.7 (CH), 130.9 (C_q), 130.4 (q, *J* = 32.5 Hz, C_q), 129.5 (CH), 127.8 (CH), 127.5 (CH), 126.2 (q, *J* = 3.7 Hz C_q), 125.0 (CH), 124.3 (q, *J* = 271.9 Hz, CF_3), 123.60 (CH), 123.56 (CH), 121.2 (CH), 121.1 (CH).

^{19}F NMR (470 MHz, Chloroform-*d*) δ -62.6 (CF_3).

HRMS (ESI-TOF) *m/z*: $[M+H]^+$ Calc'd for: $C_{35}H_{25}F_3N_3$ 544.1995; found: 544.1995.

***N*,*N*-Diphenyl-4-((5'-(4-(trifluoromethyl)phenyl)-[2,2'-bipyridin]-5-yl)ethynyl)aniline (L2ad)**

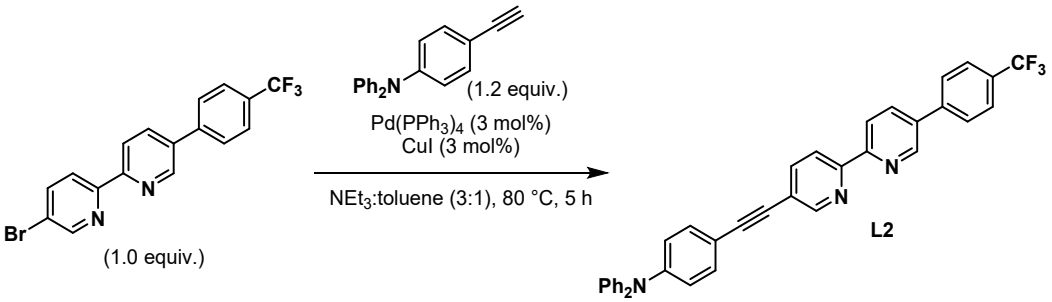

Bipyridine **4a** (45 mg, 0.12 mmol), 4-(*N*,*N*-diphenylamino)phenylacetylene (38 mg, 0.14 mmol), $Pd(PPh_3)_4$ (4.2 mg, 0.0036 mmol) and CuI (0.7 mg, 0.0036 mmol) were added to an oven-dried crimp top vial, which was evacuated and purged with N_2 three times. Dry Et_3N (0.48 mL) and toluene (0.24 mL) were added to the vial and the reaction mixture was heated to 80 °C for 5 h. The reaction mixture was then cooled to rt, diluted with saturated aq. NH_4Cl (20 mL) and extracted with CH_2Cl_2 (3 x 20 mL). The combined organic layers were dried over anhydrous Na_2SO_4. Purification by FCC (20% Et_2O in pentane) gave product **L2ad** as a yellow solid (45.9 mg, 67%).

TLC R_f = 0.30 (20% Et_2O in pentane).

^{1}H NMR (400 MHz, Chloroform-*d*) δ 8.93 (d, *J* = 2.4 Hz, 1H), 8.81 (d, *J* = 2.1 Hz, 1H), 8.53 (d, *J* = 8.2 Hz, 1H), 8.44 (d, *J* = 8.3 Hz, 1H), 8.04 (dd, *J* = 8.2, 2.4 Hz, 1H), 7.93 (dd, *J* = 8.3, 2.1 Hz, 1H), 7.76 (s, 4H), 7.41 (d, *J* = 8.6 Hz, 2H), 7.33 – 7.27 (m, 4H), 7.16 – 7.12 (m, 4H), 7.12 – 7.06 (m, 2H), 7.03 (d, *J* = 8.6 Hz, 2H).

^{13}C NMR (101 MHz, Chloroform-*d*) δ 155.4 (C_q), 153.9 (C_q), 151.7 (CH), 148.6 (C_q), 147.9 (CH), 147.2 (C_q), 141.3 (C_q), 139.3 (CH), 135.5 (CH), 135.2 (C_q), 132.8 (CH), 130.4 (q, *J* = 32.4 Hz, C_q), 129.6 (CH), 127.5 (CH), 126.2 (q, *J* = 3.5 Hz, CH), 125.3 (CH), 124.2 (q, *J* = 272.3 Hz, CF_3), 124.0 (CH), 122.1 (CH), 121.4 (CH), 121.2 (C_q), 120.6 (CH), 115.1 (C_q), 94.5 (C_q), 85.8 (C_q).

^{19}F NMR (376 MHz, Chloroform-*d*) δ -62.6 (CF_3).

HRMS (ESI-TOF) *m/z*: $[M+H]^+$ Calc'd for: $C_{37}H_{25}F_3N_3$ 568.1995; found: 568.1995.

2-Bromo-5-((4-(trifluoromethyl)phenyl)ethynyl)pyridine (P3)

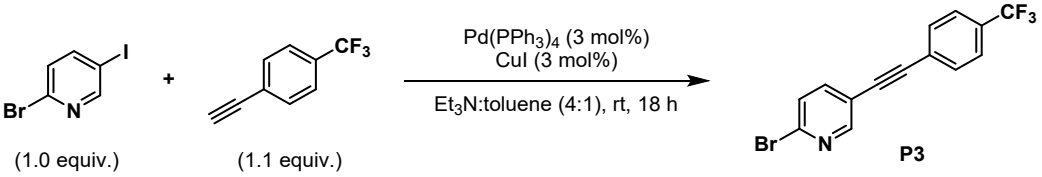

2-Bromo-5-iodopyridine (0.568 g, 2.00 mmol), $Pd(PPh_3)_4$ (69 mg, 0.06 mmol) and CuI (11 mg, 0.06 mmol) were added to an oven-dried crimp top vial, which was evacuated and purged with N_2 three times. 4-(Trifluoromethyl)phenylacetylene (0.36 mL, 2.2 mmol), dry Et_3N (4 mL) and dry toluene (1 mL) were added to the vial and the reaction mixture was stirred at rt for 18 h, then concentrated *in vacuo*. Purification by FCC (5% Et_2O in pentane) gave product **P3** as a white solid (0.465 g, 71%).

TLC R_f = 0.47 (5% Et_2O in pentane).

^{1}H NMR (500 MHz, Chloroform-*d*) δ 8.53 (d, *J* = 2.4 Hz, 1H), 7.66 (dd, *J* = 8.3, 2.4 Hz, 1H), 7.63 (s, 4H), 7.50 (d, *J* = 8.3 Hz, 1H).

^{13}C NMR (126 MHz, Chloroform-*d*) δ 152.6 (CH), 141.8 (C_q), 140.7 (CH), 132.1 (CH), 130.8 (q, *J* = 32.6 Hz, C), 127.9 (CH), 126.1 (C_q), 125.6 (q, *J* = 3.7 Hz, CH), 123.9 (q, *J* = 271.9 Hz, CF_3), 119.2 (CBr), 92.5 (C_q), 87.1 (C_q).

^{19}F NMR (376 MHz, Chloroform-*d*) δ -62.9 (CF_3).

HRMS (ESI-TOF) *m/z*: $[M+H]^+$ Calc'd for: $C_{14}H_7BrF_3N$ 325.9787, 327.9767; found: 325.9786, 327.9765.

5-Bromo-5'-((4-(trifluoromethyl)phenyl)ethynyl)-2,2'-bipyridine (4b)

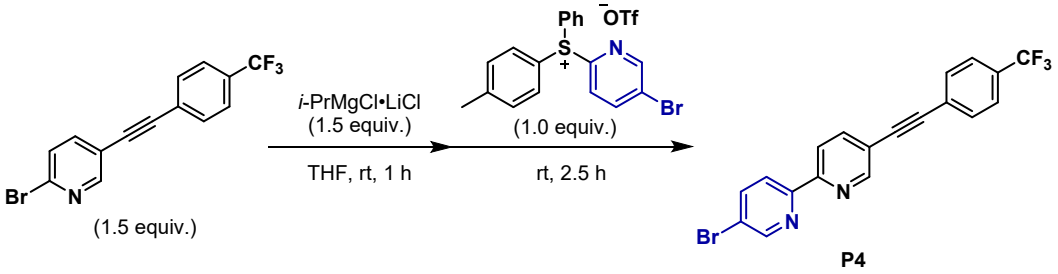

Product **4b** was synthesised *via* general procedure A using **P3** (0.23 g, 0.69 mmol) and bromopyridyl sulfonium salt **1** (0.233 g, 0.460 mmol). The Grignard reagent was formed at rt for 1 h and the ligand coupling reaction was stirred at rt for 2.5 h. Purification by FCC (5% Et_2O in pentane) gave bipyridine **4b** as a white solid (89.2 mg, 48%).

TLC R_f = 0.38 (5% Et_2O in pentane).

^{1}H NMR (400 MHz, Chloroform-*d*) δ 8.81 (d, *J* = 2.0 Hz, 1H), 8.73 (d, *J* = 2.3 Hz, 1H), 8.41 (d, *J* = 8.2 Hz, 1H), 8.35 (d, *J* = 8.5 Hz, 1H), 7.97 – 7.95 (m, 1H), 7.95 – 7.93 (m, 1H), 7.72 – 7.61 (m, 4H).

^{13}C NMR (126 MHz, Chloroform-*d*) δ 154.5 (C_q), 153.9 (C_q), 151.9 (CH), 150.5 (CH), 139.7 (CH), 132.1 (CH), 130.7 (q, *J* = 32.8 Hz, C_q), 126.5 (C_q), 125.6 (q, *J* = 3.7 Hz, CH), 124.0 (q, *J* = 272.0 Hz, CF_3), 122.8 (CH), 121.7 (CBr), 120.4 (CH,), 120.0 (C_q), 92.3 (C_q), 88.7 (C_q).

^{19}F NMR (376 MHz, Chloroform-*d*) δ -62.9 (CF_3).

HRMS (ESI-TOF) *m/z*: $[M+H]^+$ Calc'd for: $C_{19}H_{11}BrF_3N_2$ 403.0052, 405.0034; found: 403.0050, 405.0031.

***N*,*N*-Diphenyl-4-(5'-((4-(trifluoromethyl)phenyl)ethynyl)-[2,2'-bipyridin]-5-yl)aniline L3bc**

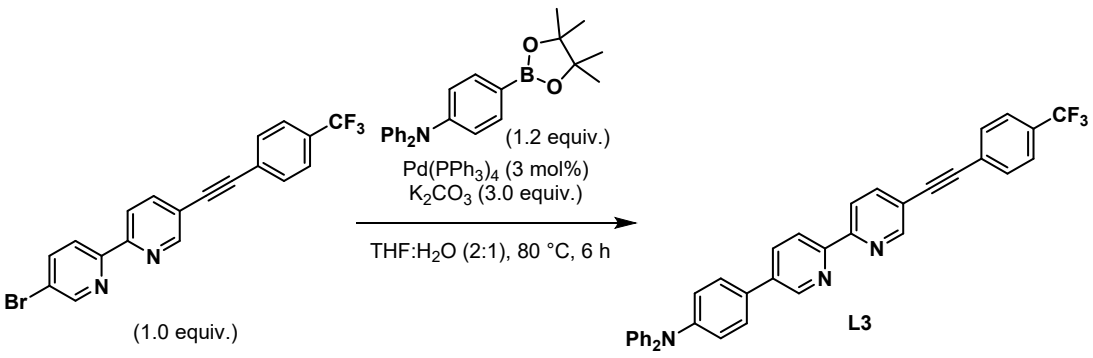

Bipyridine **4b** (46 mg, 0.11 mmol), *N*,*N*-diphenyl-4-(4,4,5,5-tetramethyl-1,3,2-dioxaborolan-2-yl)aniline (52 mg, 0.14 mmol), K_2CO_3 (46 mg, 0.33 mmol) and $Pd(PPh_3)_4$ (3.8 mg, 0.0033 mmol) were added to an oven-dried crimp top vial, which was evacuated and purged with N_2 three times. THF (0.36 mL) and H_2O (0.18 mL) were added to the vial and the reaction mixture was heated to 80 °C for 6 h. The reaction mixture was then cooled to rt, diluted with H_2O (20 mL) and extracted with CH_2Cl_2 (3 x 20 mL). The combined organic layers were dried over anhydrous Na_2SO_4. Purification by FCC (10% Et_2O in pentane) gave product **L3bc** as a yellow solid (42.9 mg, 69%).

TLC R_f = 0.12 (10% Et_2O in pentane).

^{1}H NMR (400 MHz, Chloroform-*d*) δ 8.92 (d, *J* = 2.4 Hz, 1H), 8.84 (d, *J* = 2.1 Hz, 1H), 8.47 (d, *J* = 8.3 Hz, 1H), 8.46 (d, *J* = 8.3 Hz, 1H), 8.00 (dd, *J* = 8.3, 2.4 Hz, 1H), 7.96 (dd, *J* = 8.3, 2.1 Hz, 1H), 7.70 – 7.62 (m, 4H), 7.54 (d, *J* = 8.6 Hz, 2H), 7.33 – 7.27 (m, 4H), 7.22 – 7.12 (m, 6H), 7.11 – 7.04 (m, 2H).

^{13}C NMR (101 MHz, Chloroform-*d*) δ 155.3 (C_q), 153.6 (C_q), 151.9 (CH), 148.4 (C_q), 147.5 (C_q), 147.4 (CH), 139.6 (CH), 136.5 (C_q), 134.6 (CH), 132.1 (CH), 130.8 (C_q), 130.6 (q, *J* = 33.1 Hz, C_q), 129.6 (CH), 127.9 (CH), 126.6 (C_q), 125.6 (q, *J* = 3.5 Hz, CH), 125.0 (CH), 124.0 (q, *J* = 272.3 Hz, CF_3), 123.58 (CH), 123.56 (CH), 121.5 (CH), 120.4 (CH), 119.5 (C_q), 92.1 (C_q), 88.9 (C_q).

^{19}F NMR (376 MHz, Chloroform-*d*) δ -62.8 (CF_3).

HRMS (ESI-TOF) *m/z*: $[M+H]^+$ Calc'd for: $C_{37}H_{25}F_3N_3$ 568.1995; found: 568.1995.

3.0 Complex Synthesis

The complexation reactions of the ligand series were adapted from common literature procedures.[1] The Ru(bipyridine)$_2$Cl$_2$ precursor was synthesised according to literature procedures from $RuCl_3.xH_2O$ and 2,2'-bipyridine which were purchased from Fisher Scientific and used without further purification. Ethylene glycol was purchased from Fisher Scientific. Solvents were dried using appropriate drying agents (sodium, molecular sieves, or $MgSO_4$), and distilled under a nitrogen atmosphere. Flash chromatography was performed using silica gel 60 (Sigma Aldrich/Merck), particle size 40-63 µm as the stationary phase.

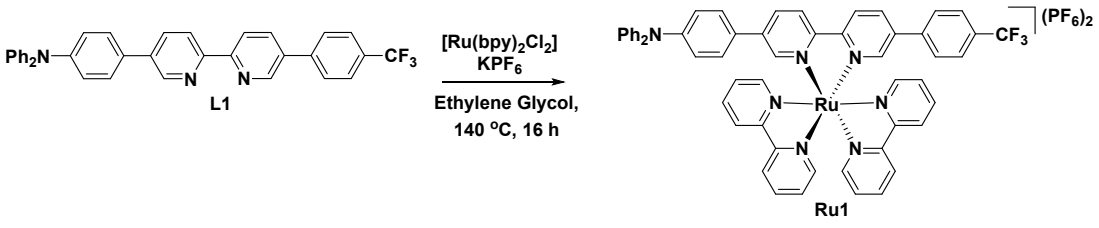

[Ru(2, 2'-bipyridine)$_2$(L1ac)][(PF$_6$)$_2$] (Ru1)

Ru(bpy)$_2$Cl$_2$ (30 mg, 0.06 mmol) , and **L1ac** (34 mg, 0.06 mmol)were dissolved in ethylene glycol and the reaction mixture heated to 140 °C for 16 h under Argon. After cooling, saturated aqueous KPF_6 was added until a precipitate formed (3 mL) and the resulting precipitate isolated by filtration. The crude product was purified

using column chromatography (silica, MeCN, H_2O, sat. KNO_3, 90:9:1 v/v) followed by precipitation by saturated aqeous KPF_6 and recrystallised from MeOH and Et_2O to yield **Ru1** (50 mg, 65% yield).

^{1}H NMR (600 MHz, CD_3CN) δ 8.57 (d, *J* = 8.5 Hz, 1H), 8.53 (d, *J* = 8.6 Hz, 1H), 8.51-8.44 (m, 4H), 8.32 (dd, *J* = 8.5, 2.1 Hz, 1H), 8.26 (dd, *J* = 8.6, 2.1 Hz, 1H), 8.12-8.01 (m, 4H), 7.88 (t, *J* = 5.5 Hz, 2H), 7.82-7.72 (m, 6H), 7.58 (d, *J* = 8.2 Hz, 2H), 7.46-7.38 (m, 4H), 7.38-7.31 (m, 4H), 7.29 – 7.23 (m, 2H), 7.20-7.12 (m, 2H), 7.12-7.03 (m, 4H), 6.98- 6.92 (m, 2H)

^{13}C NMR (151 MHz, CD_3CN) δ, 158.08 (C_q), 158.06 (C_q), 157.93 (C_q), 157.86 (C_q), 157.28 (C_q), 155.03 (C_q), 153.03 (CH), 152.98 (C_q), 152.89 (CH), 152.81 (CH) 150.55 (CH), 150.30 (C_q), 148.97 (CH), 147.75 (C_q), 140.33 (C_q), 139.85 (C_q), 139.10 (C_q), 138.90 (CH), 138.82 (C_q), 138.76 (CH), 138.74 (C_q), 137.06 (CH), 135.35 (CH), 131.42 (C_q), 130.67 (CH), 128.89 (CH), 128.69 (CH), 128.56 (C_q), 128.52 (CH), 128.49 (C_q), 127.54 (C_q), 127.06 (CH), 126.48 (CH), 125.46 (CH), 125.43 (CH), 125.39 (CH), 125.36 (CH), 125.26 (CH), 125.22 (CH), 124.93 (CH), 122.38 (CH).

HRMS (m/z, APCI$^+$, MeOH) $[M-(PF_6)_2]^{2+}$, $(C_{55}H_{40}F_3N_7Ru)^{2+}$, Calculated mass: 478.617229; Found: 478.618508.

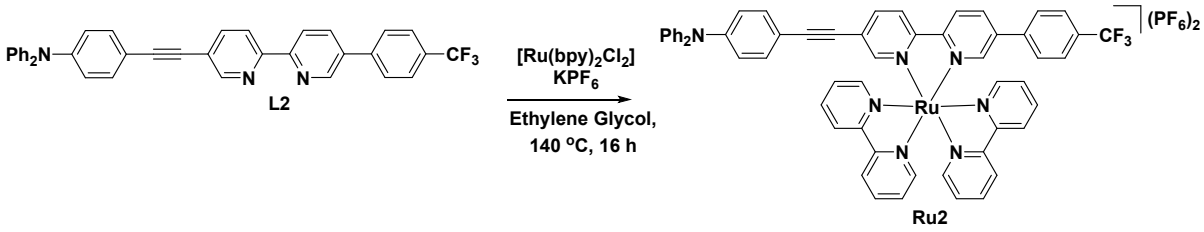

[Ru(2, 2'-bipyridine)$_2$(L2ad)][(PF$_6$)$_2$] (Ru2)

$Ru(bpy)_2Cl_2$ (28 mg, 0.05 mmol) , and **L2ad** (30 mg, 0.05 mmol) were dissolved in ethylene glycol and the reaction mixture heated to 140 °C for 16 h under Argon. After cooling, saturated aqueous KPF_6 was added until a precipitate formed (3 mL) and the resulting precipitate isolated by filtration. The crude product was purified using column chromatography (silica, MeCN, H_2O, sat. KNO_3, 90:9:1 v/v) followed by precipitation by saturated aqueous KPF_6 and recrystallised from MeOH and Et_2O to yield **Ru2** (25 mg, 38% yield).

^{1}H NMR (600 MHz, CD_3CN) δ 8.56 (d, J = 8.6 Hz, 1H), 8.53-8.45 (m, 5H), 8.32 (dd, J = 8.5, 2.0 Hz, 1H), 8.11 (dd, J = 8.5, 1.8 Hz, 1H), 8.10-8.02 (m, 4H), 7.84 (dd, J = 9.0, 5.7 Hz, 2H), 7.80 (dd, J = 7.4, 1.8 Hz, 2H), 7.77-7.69 (m, 4H), 7.57 (d, J = 8.3 Hz, 2H), 7.46-7.38 (m, 4H), 7.38-7.32 (m, 4H), 7.32-7.28 (m, 2H), 7.16 (dd, J = 11.6, 4.2 Hz, 2H), 7.14-7.09 (m, 4H), 6.93 – 6.89 (m, 2H).

^{13}C NMR (151 MHz, CD_3CN) δ 158.02 (C_q), 157.98 (C_q), 157.96 (C_q), 156.98 (C_q), 155.91 (C_q), 154.00 (CH), 153.15 (CH), 153.01 (CH), 152.84 (CH), 152.76 (CH), 150.55 (CH), 150.47 (C_q), 147.63 (CH), 140.24 (CH), 138.99 (CH), 138.96 (CH), 138.93 (CH), 137.13 (CH), 133.83 (CH), 130.74 (CH), 128.98 (CH), 128.66 (CH), 128.62 (C_q), 128.52

(C_q), 127.12 (C_q), 126.69 (CH), 125.63 (CH), 125.51 (CH), 125.49 (C_q), 125.40 (CH), 125.33 (CH), 125.14 (CH), 121.59 (CH), 118.31 (C_q), 98.67 (C_q), 84.51 (C_q).

HRMS (m/z, APCI$^+$, MeOH) $[M-(PF_6)_2]^{2+}$ $(C_{57}H_{40}F_3N_7Ru)^{2+}$, Calculated mass: 490.617527; Found: 490.618130.

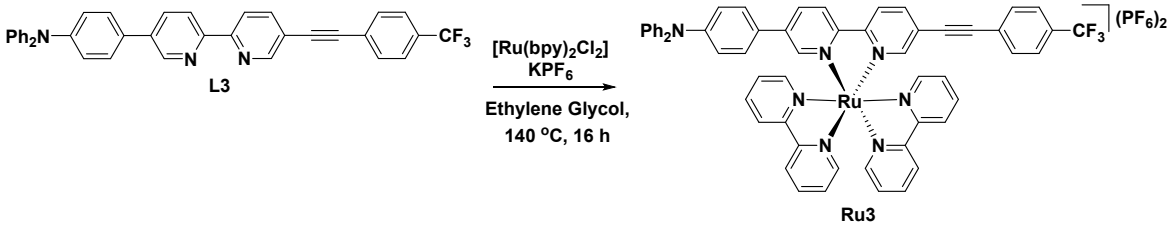

[Ru(2, 2'-bipyridine)$_2$(L3bc)][(PF_6)$_2$] (Ru3)

$Ru(bpy)_2Cl_2$ (28 mg, 0.05 mmol) and **L3bc** (30 mg, 0.05 mmol) were dissolved in ethylene glycol and the reaction mixture heated to 140 °C for 16 h under Argon. After cooling, saturated aqueous KPF_6 was added until a precipitate formed (3 mL) and the resulting precipitate isolated by filtration. The crude product was purified using column chromatography (silica, MeCN, H_2O, sat. KNO_3, 90:9:1 v/v) followed by precipitation by saturated aqueous KPF_6 and recrystallised from MeOH and Et_2O to yield **Ru2** (10 mg, 15% yield)

^{1}H NMR (600 MHz, CD_3CN) δ 8.50 (m, 6H), 8.25 (dd, J = 8.6, 2.1 Hz, 1H), 8.17 (dd, J = 8.5, 1.8 Hz, 1H), 8.10-8.02 (m, 4H), 7.88 (d, J = 1.6 Hz, 1H), 7.84 (dd, J = 15.4, 5.2 Hz, 2H), 7.76-7.71 (m, 5H), 7.65 (m, J = 8.2 Hz, 2H), 7.45-7.37 (m, 4H), 7.37-7.33 (m, 4H), 7.27-7.22 (m, 2H), 7.18 – 7.14 (m, 2H), 7.08 (dd, J = 8.5, 1.0 Hz, 4H), 6.95-6.92 (m, 2H).

^{13}C NMR (151 MHz, CD_3CN) δ 157.05 (C_q), 156.99 (C_q), 156.89 (C_q), 156.35 (C_q), 153.82 (CH), 153.42 (CH), 152.12 (CH), 152.00 (CH), 151.81 (CH), 151.79 (CH), 149.66 (C_q), 148.13 (CH), 146.76 (C_q), 139.84 (CH), 139.49 (C_q), 138.04 (CH), 137.94 (CH), 134.34 (CH), 132.24 (CH), 130.59 (C_q), 129.73 (CH), 127.75 (CH), 127.66 (CH), 127.61 (CH), 127.56 (CH), 126.46 (C_q), 125.73 (CH), 125.57 (CH), 124.79 (CH), 124.52 (CH), 124.46 (CH), 124.41 (CH), 124.38 (CH), 124.29 (CH), 123.60 (CH), 122.68 (C_q), 121.35 (CH), 94.21 (C_q), 86.14 (C_q).

HRMS (m/z, APCI$^+$, MeOH) $[M-(PF_6)_2]^{2+}$, $(C_{57}H_{40}F_3N_7Ru)^{2+}$, Calculated mass: 490.617527; Found: 490.618130.

4.0 Spectroscopic Structural Characterisation

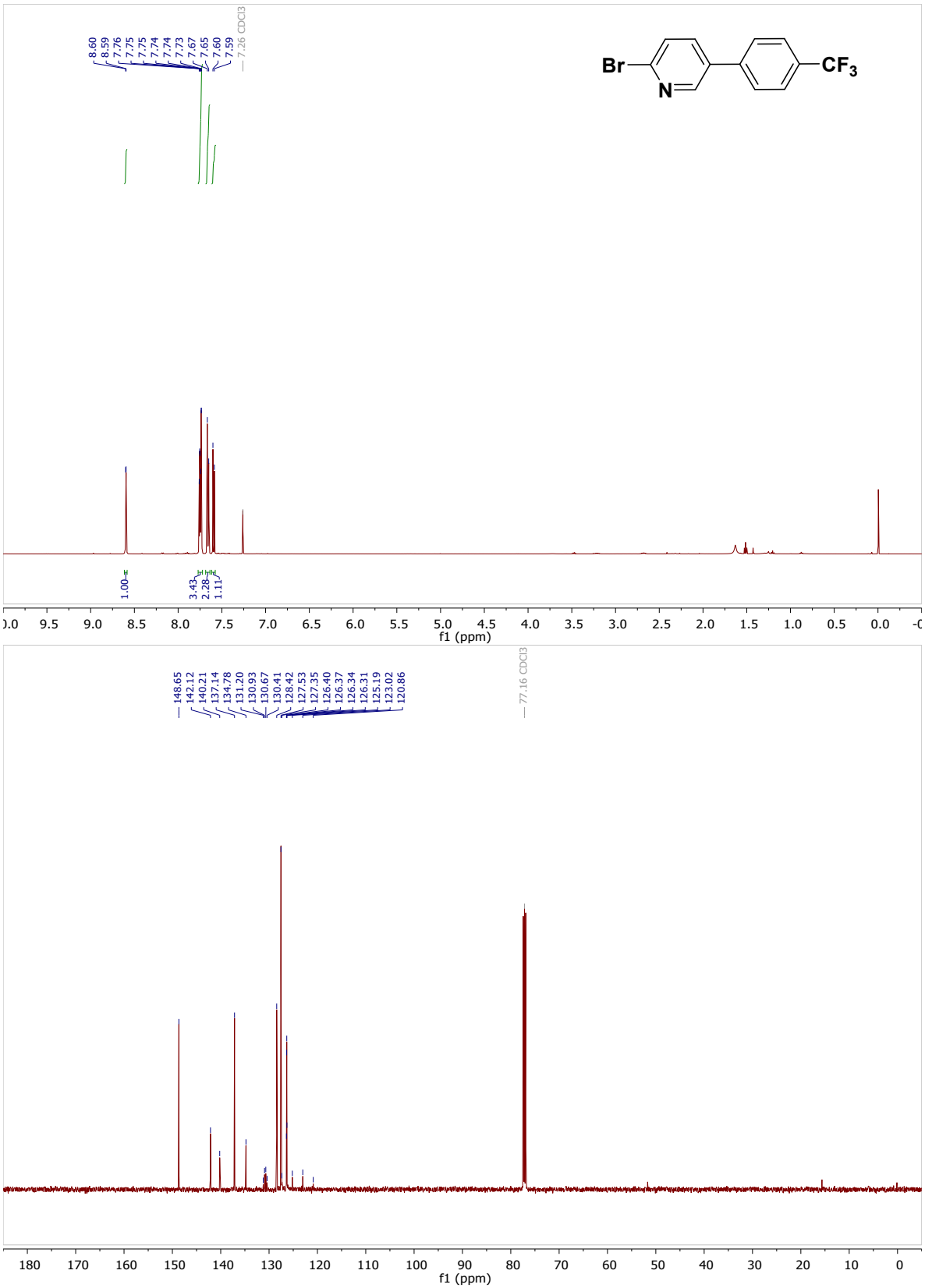

Figure S1 . ^{1}H (400 MHz) and ^{13}C (101 MHz) NMR spectra of **P1** in $CDCl_3$

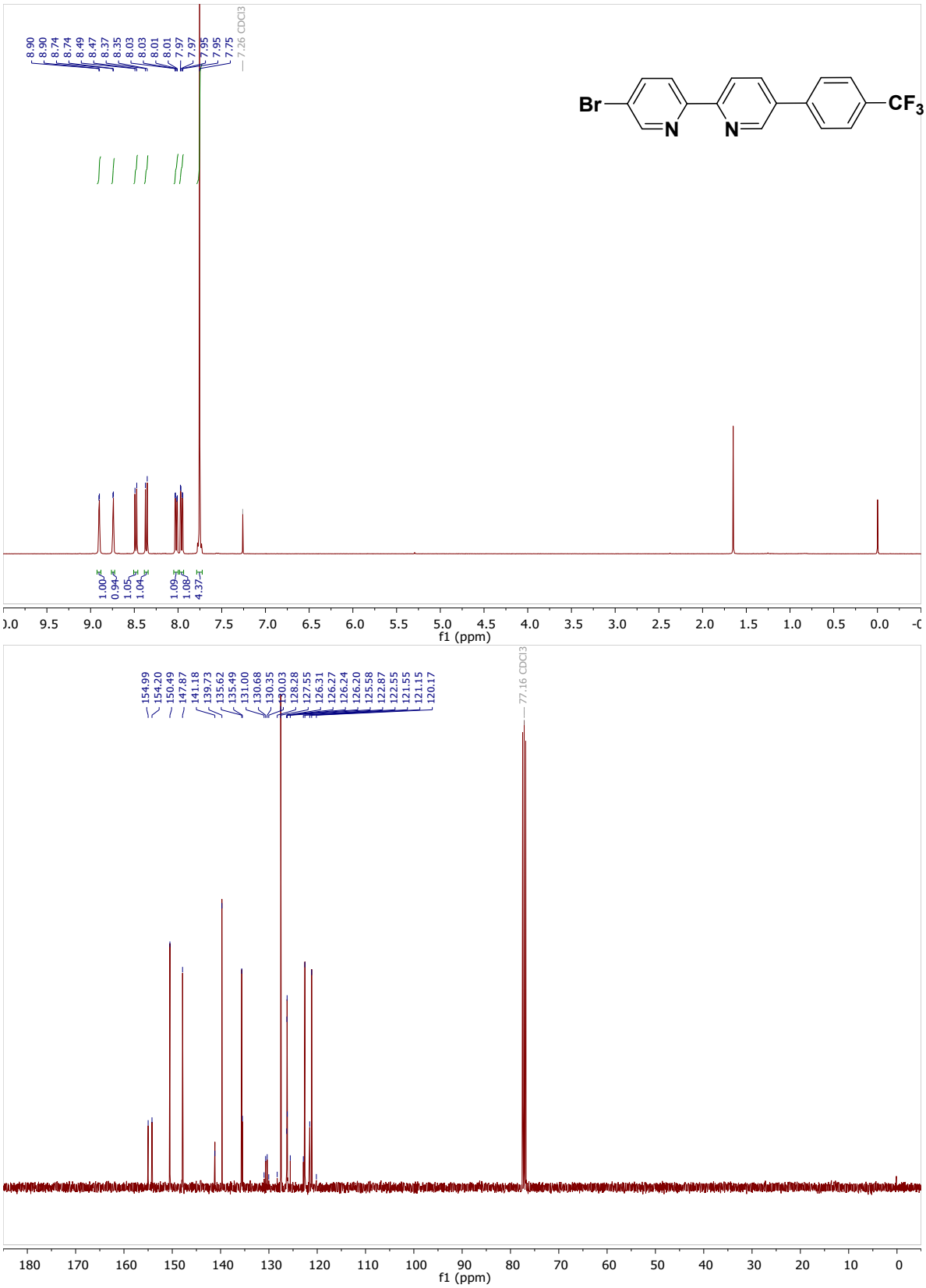

Figure S2. ^{1}H (400 MHz) and ^{13}C (101 MHz) NMR spectra of **4b** in $CDCl_3$

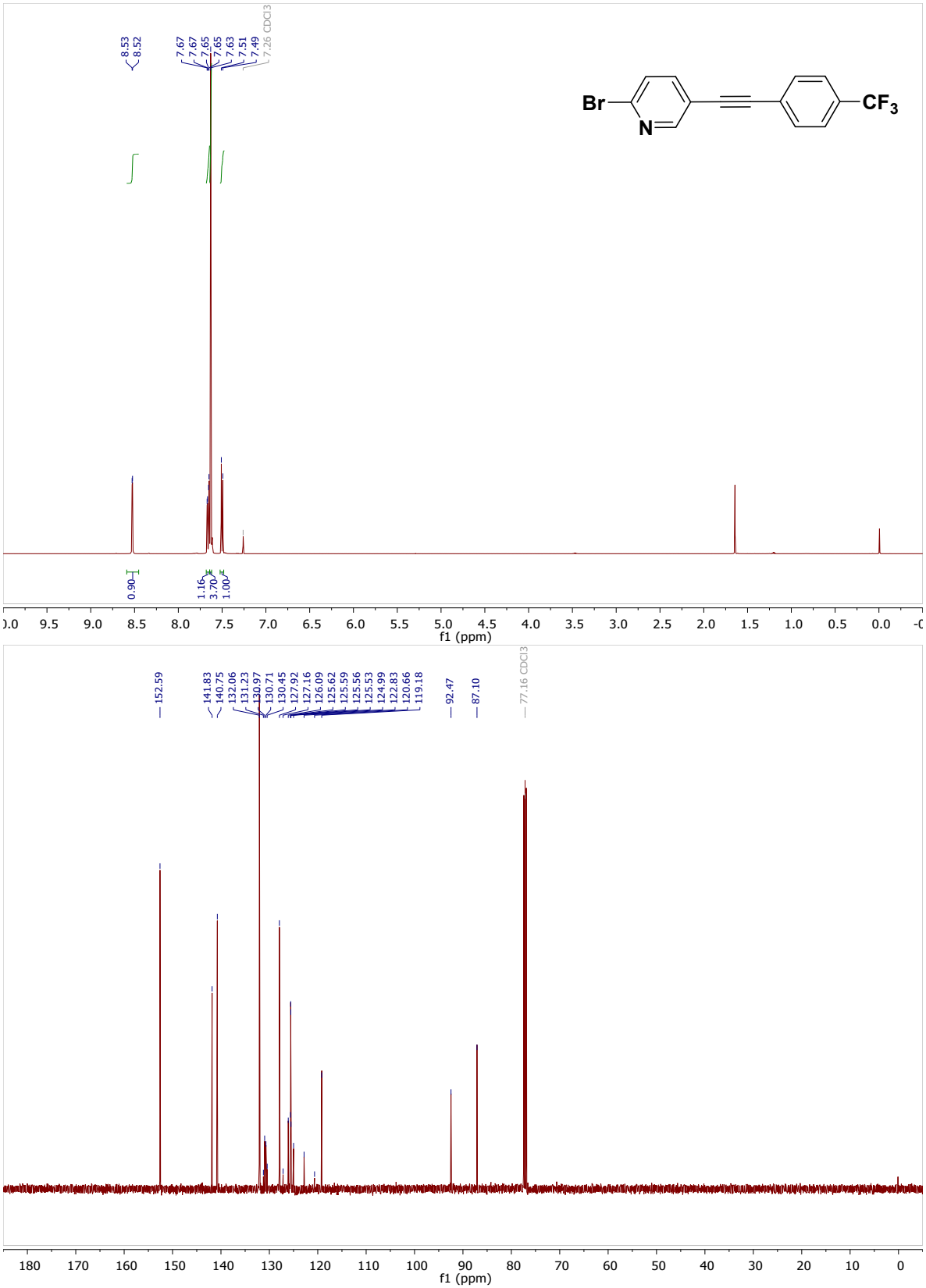

Figure S3. ^{1}H (400 MHz) and ^{13}C (101 MHz) NMR spectra of **P3** in $CDCl_3$

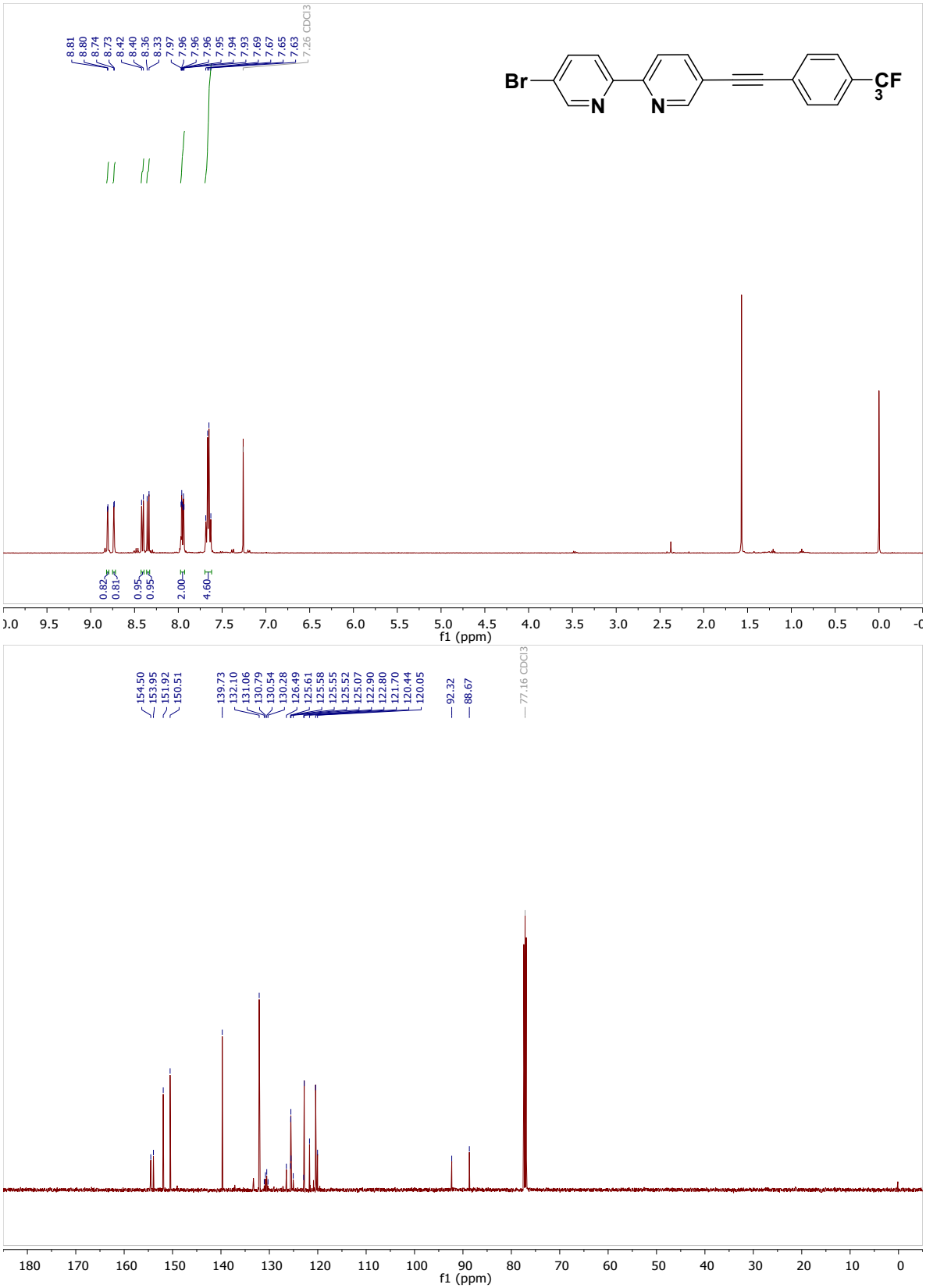

Figure S4. ^{1}H (400 MHz) and ^{13}C (101 MHz) NMR spectra of **4a** in $CDCl_3$

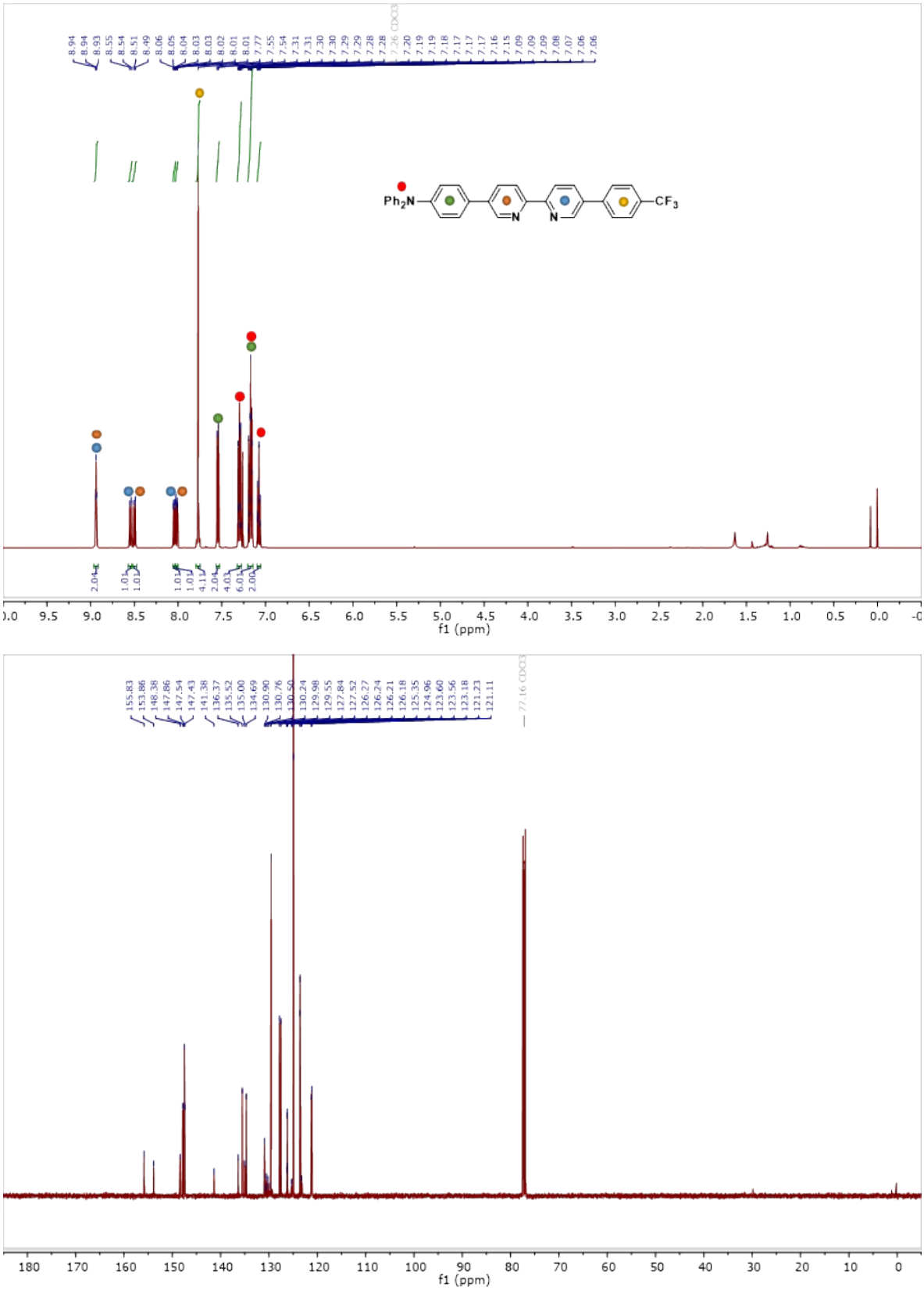

Figure S5. ^{1}H (400 MHz) and ^{13}C (101 MHz) NMR spectrum of **L1ac** in $CDCl_3$

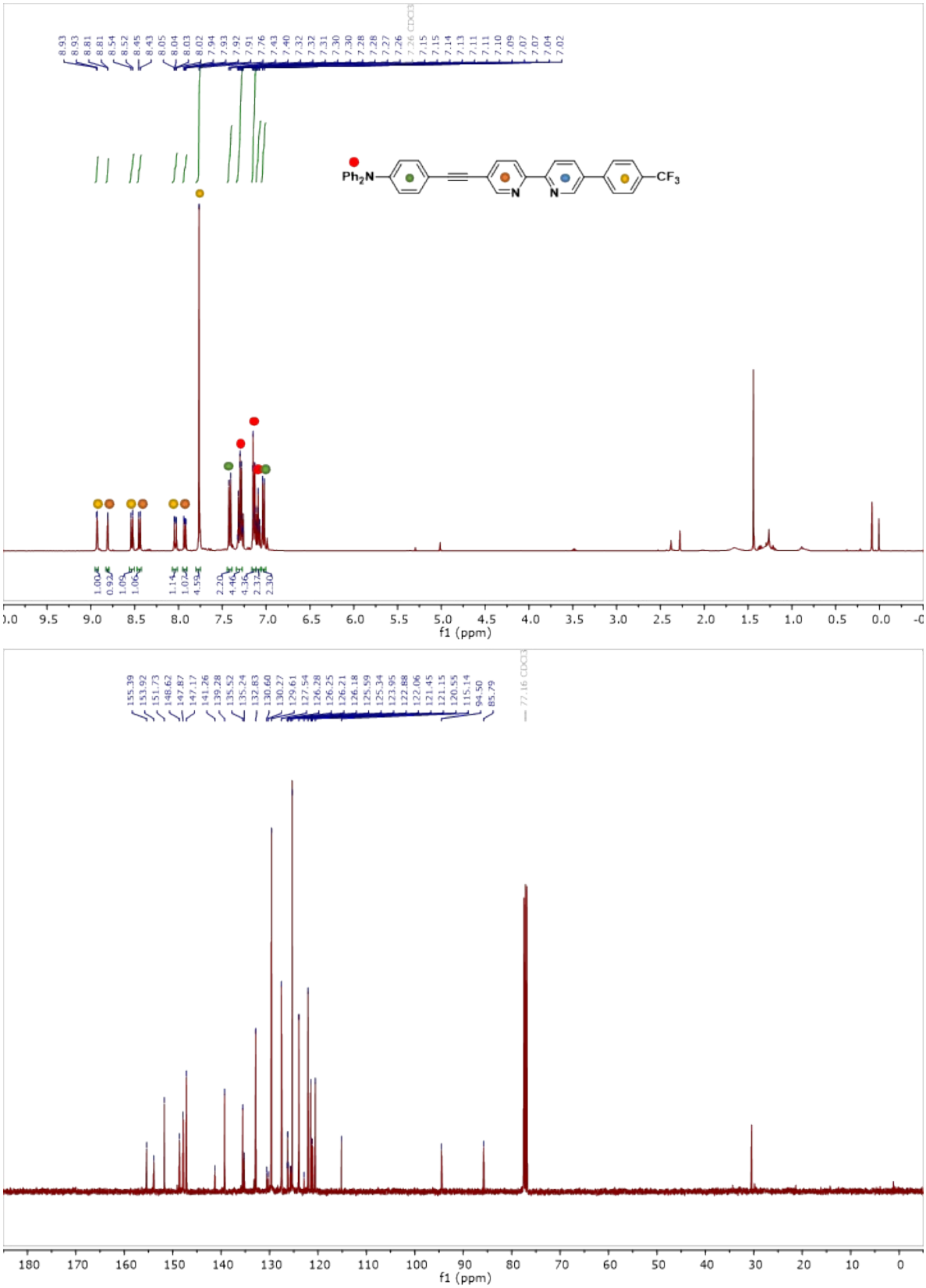

Figure S6. ^{1}H (400 MHz) and ^{13}C (101 MHz) NMR spectrum of **L2ad** in $CDCl_3$

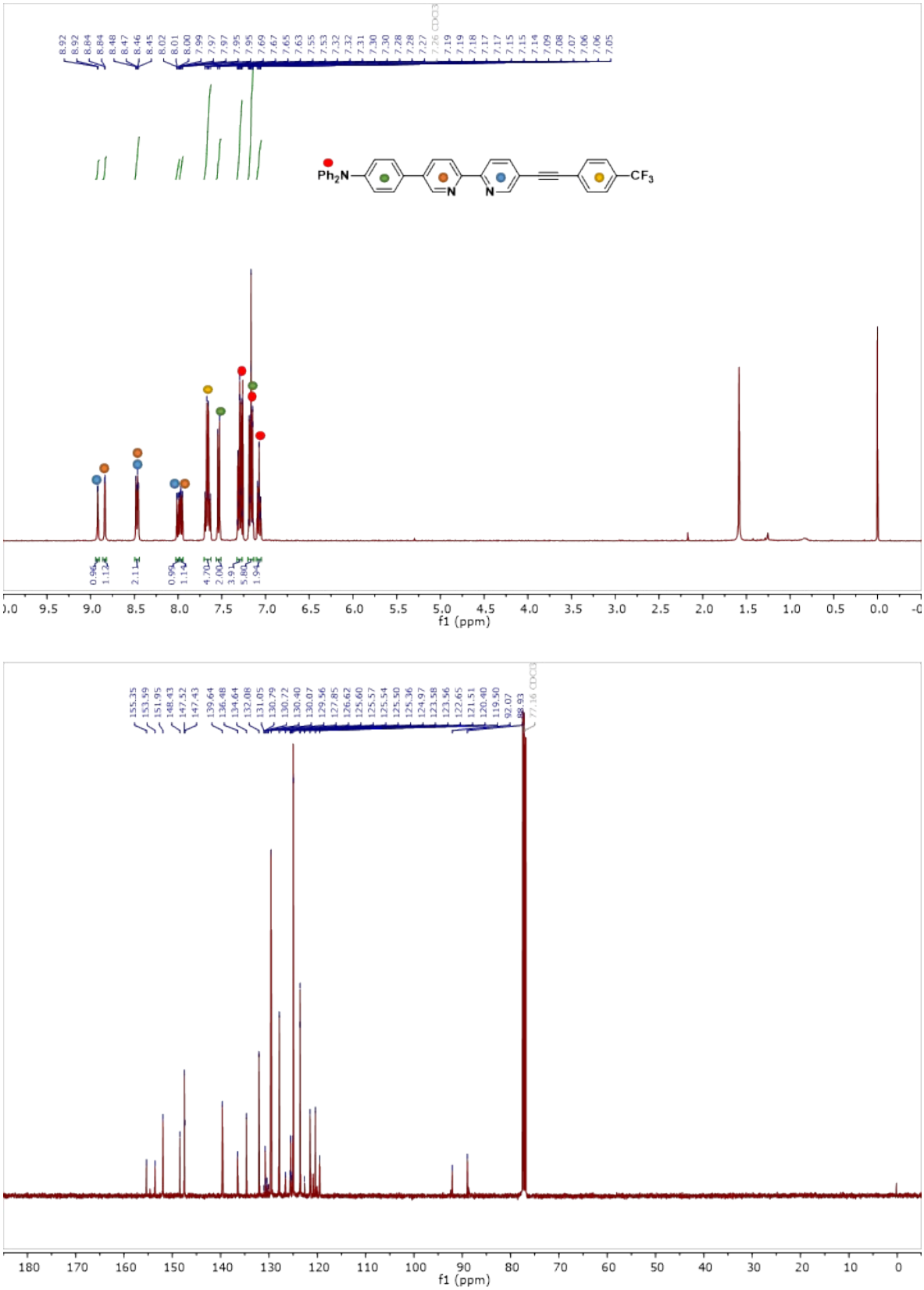

Figure S7. ^{1}H (400 MHz) and ^{13}C (101 MHz) NMR spectrum of **L3bc** in $CDCl_3$

A)

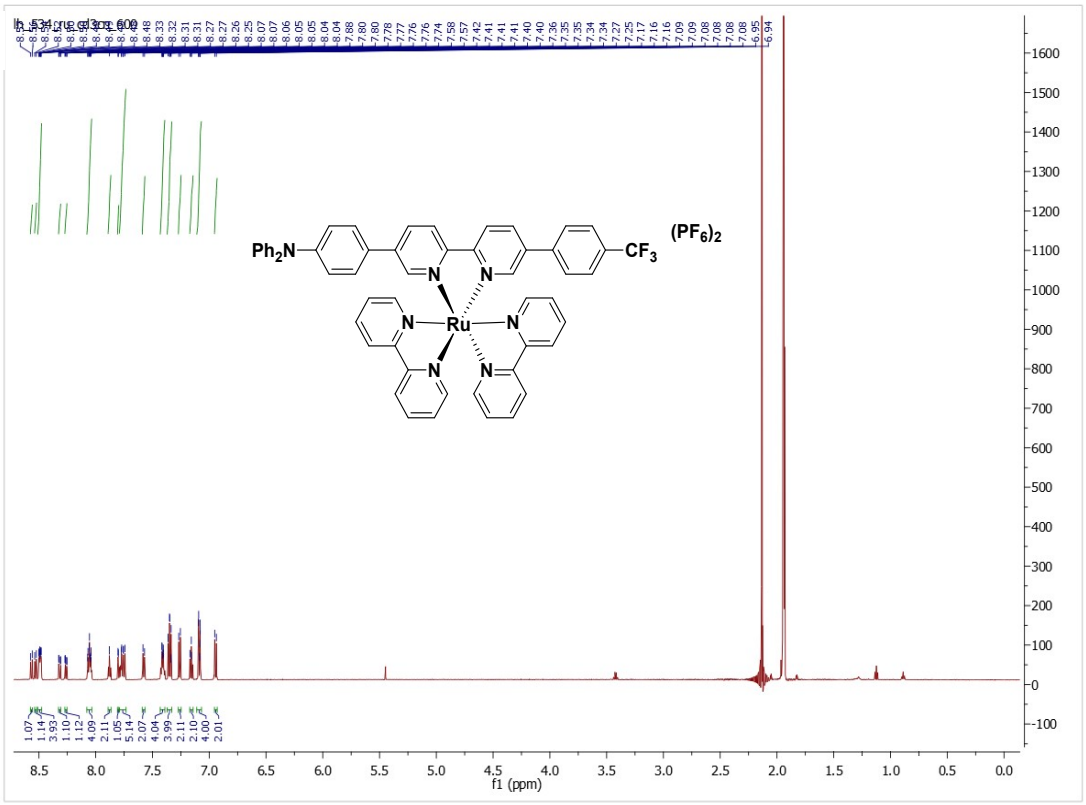

B)

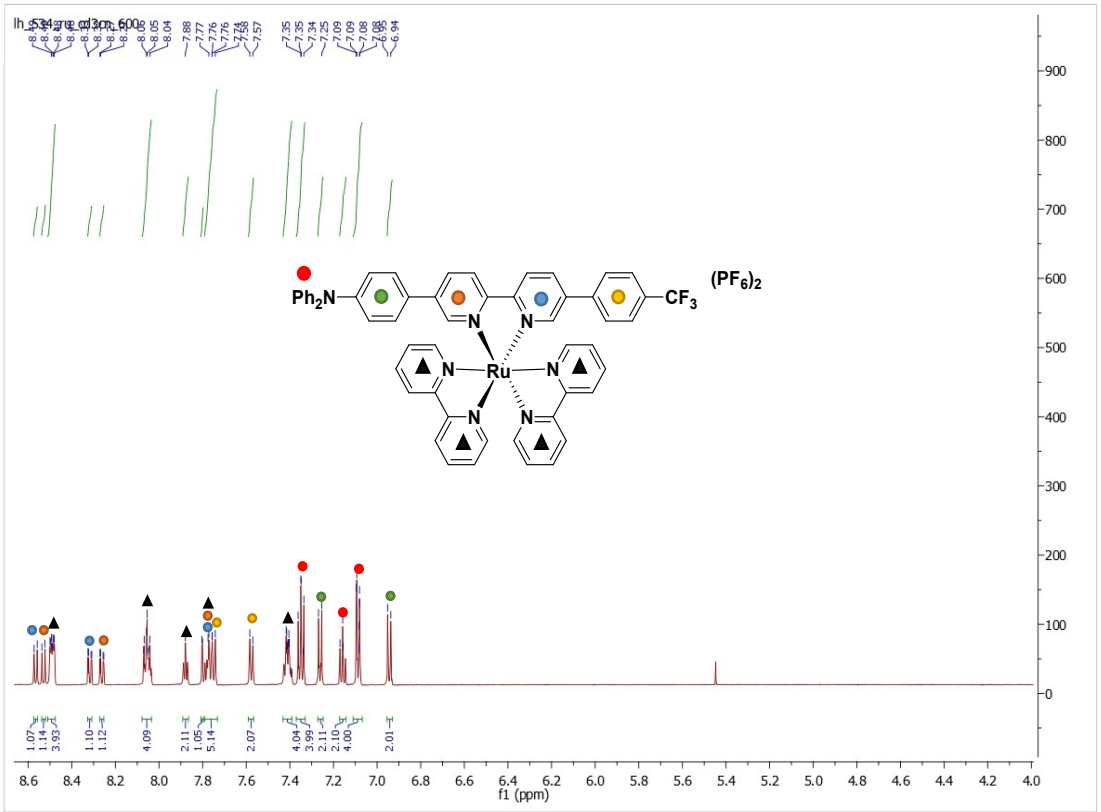

Figure S8. A) Assigned ^{1}H NMR spectrum of **Ru1** (Acetonitrile-d_3 600 MHz) B) inset of aromatic region (4 – 8.6 ppm)

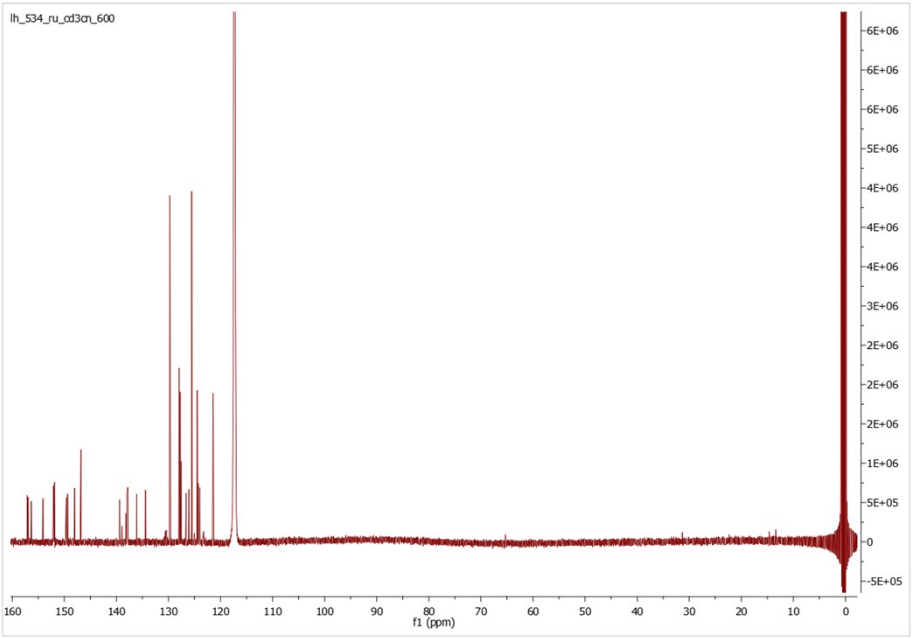

Figure S9. ^{13}C NMR Spectrum of **Ru1** (MeCN-d_3 150 MHz)

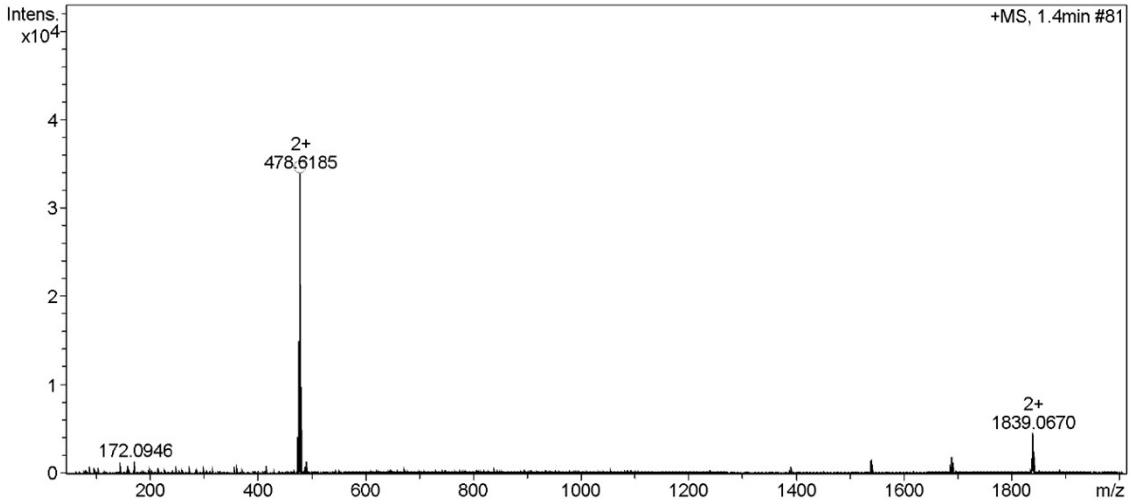

Meas. m/z	#	Ion Formula	m/z	err [mDa]	err [ppm]	rdb	N-Rule	e⁻ Conf	mSigma
478.618508	1	C55H40F3N7Ru	478.617229	-1.3	-2.7	38.5	-	odd	13.6

Figure S10. ESI HRMS for **Ru1**

A)

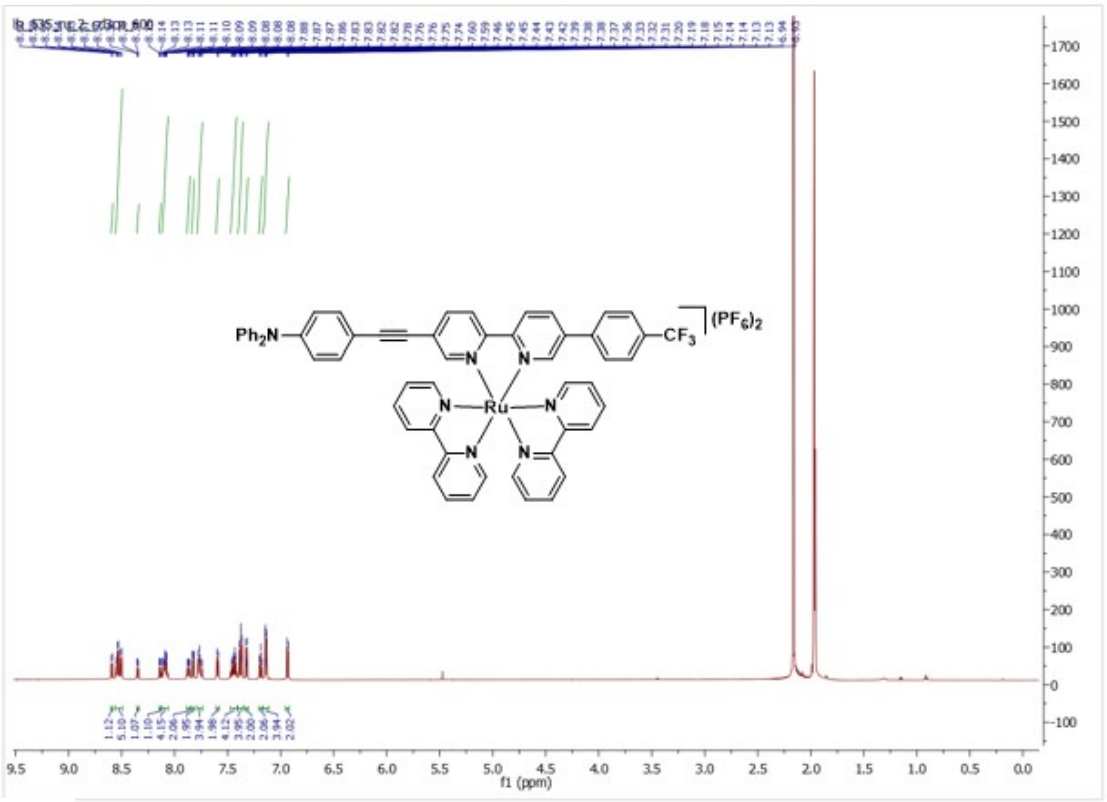

B)

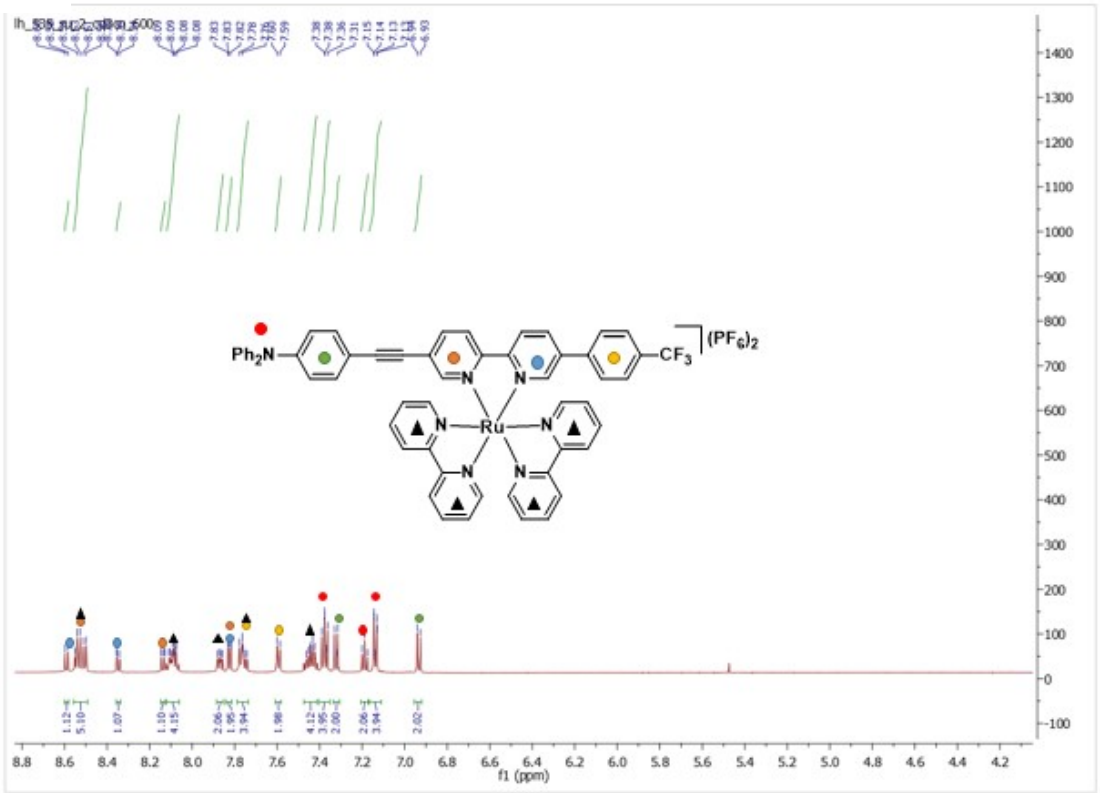

Figure S11. A) Assigned ^{1}H NMR spectrum of **Ru2** (Acetonitrile-d_3 600 MHz) B) inset of aromatic region (4 – 8.6 ppm)

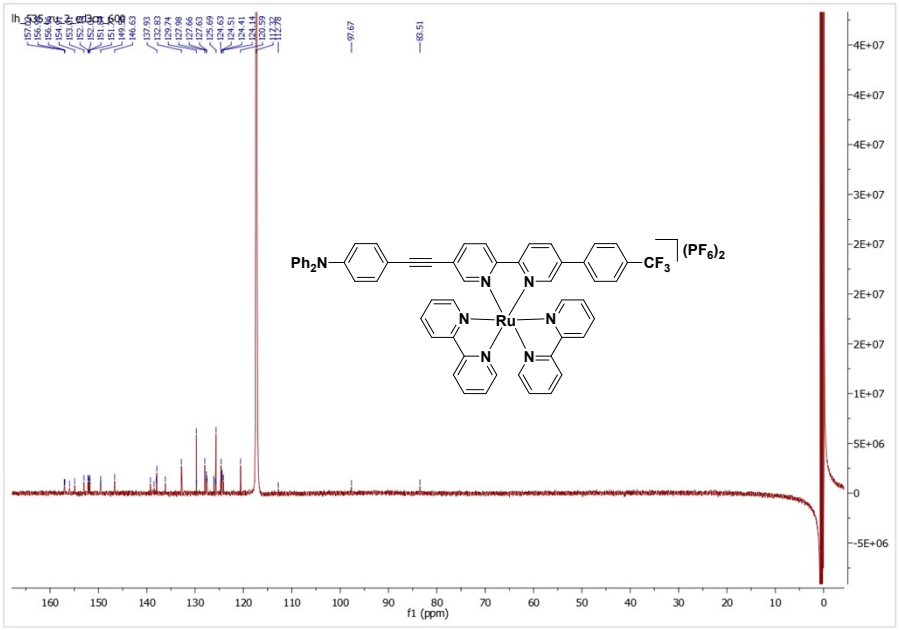

Figure S12. ^{13}C NMR Spectrum of **Ru2** (MeCN-d_3 150 MHz)

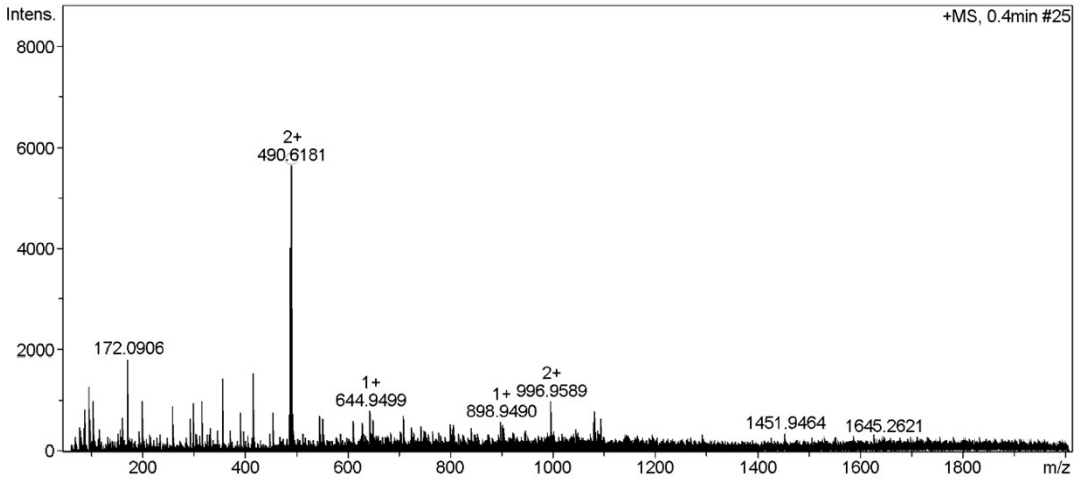

Meas. m/z	#	Ion Formula	m/z	err [mDa]	err [ppm]	rdb	N-Rule	e⁻ Conf	mSigma
490.618130	1	C57H40F3N7Ru	490.617257	0.9	1.8	40.5	-	odd	50.7

Figure S13. ESI HRMS for **Ru2**

A)

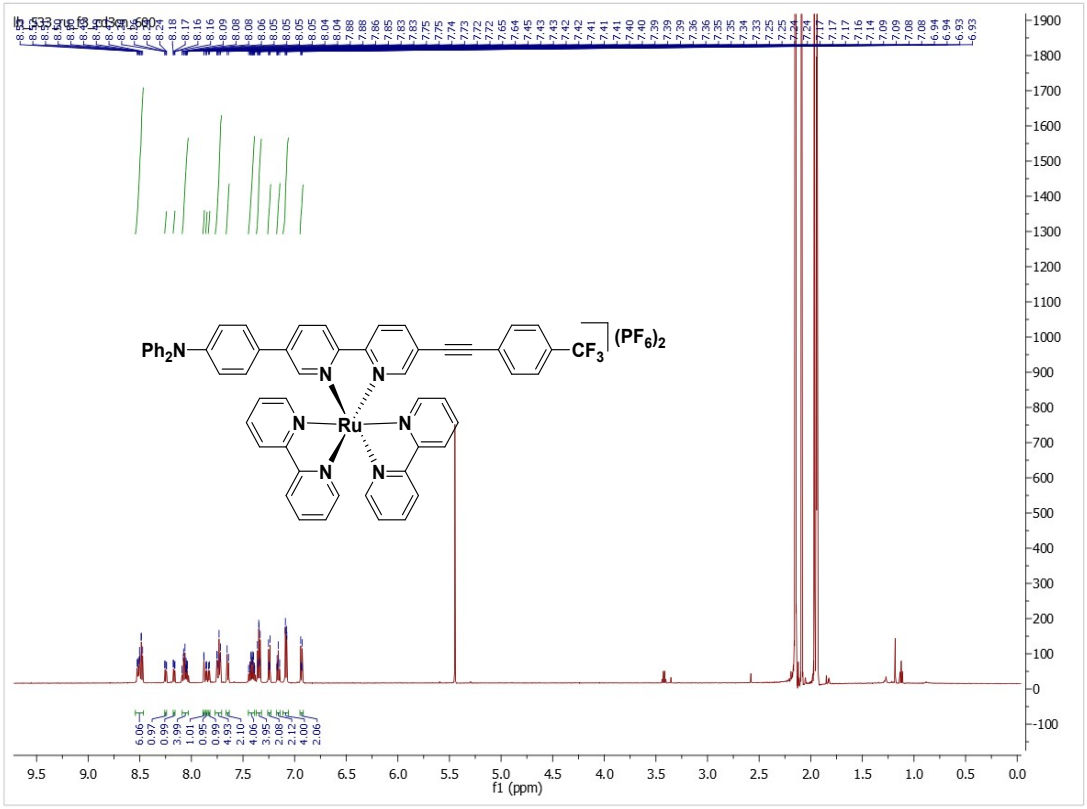

B)

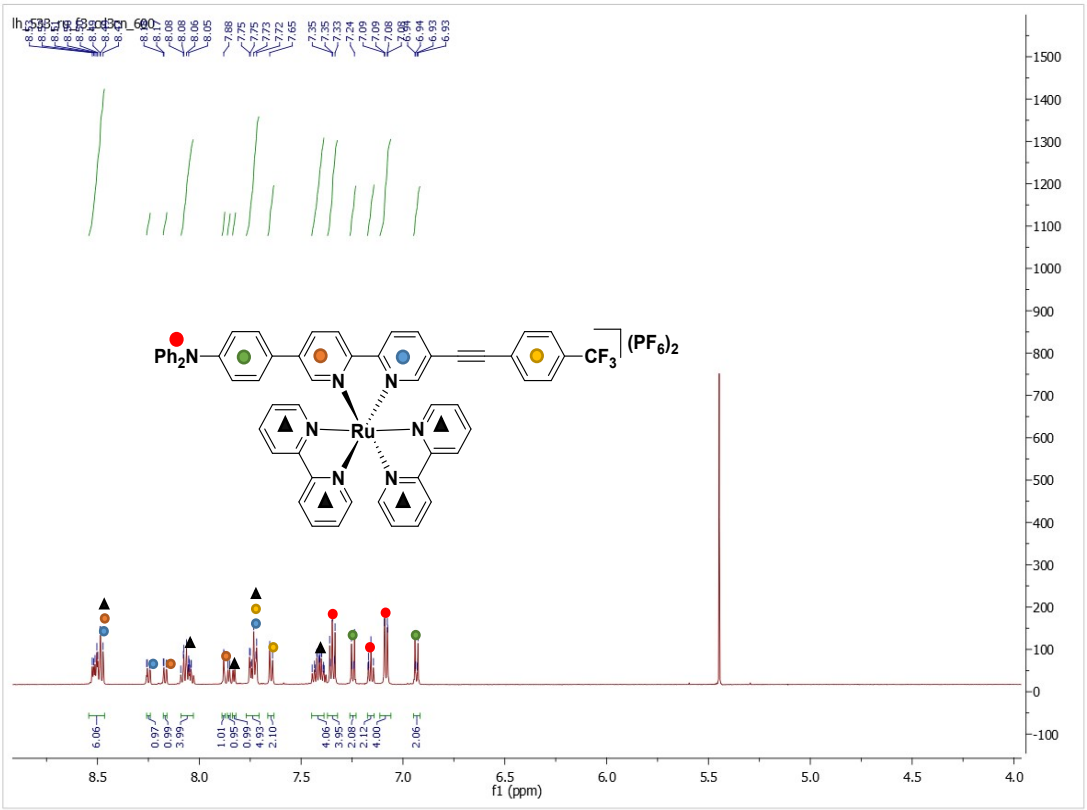

Figure S14. A) Assigned ^{1}H NMR spectrum of **Ru3** (Acetonitrile-d_3 600 MHz) B) inset of aromatic region (4 – 8.6 ppm)

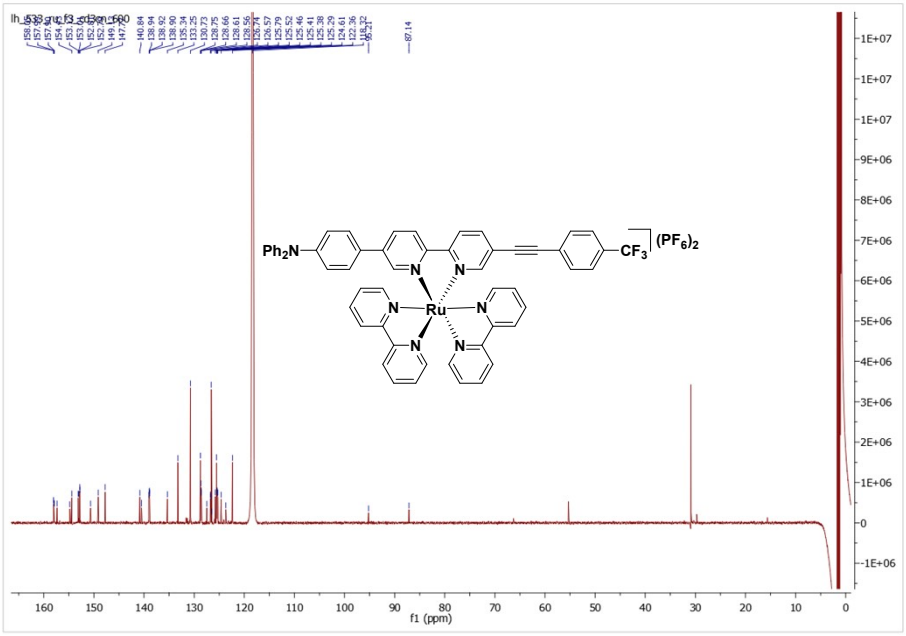

. **Figure S15.** ^{13}C NMR Spectrum of **Ru3** (MeCN-d_3 150 MHz)

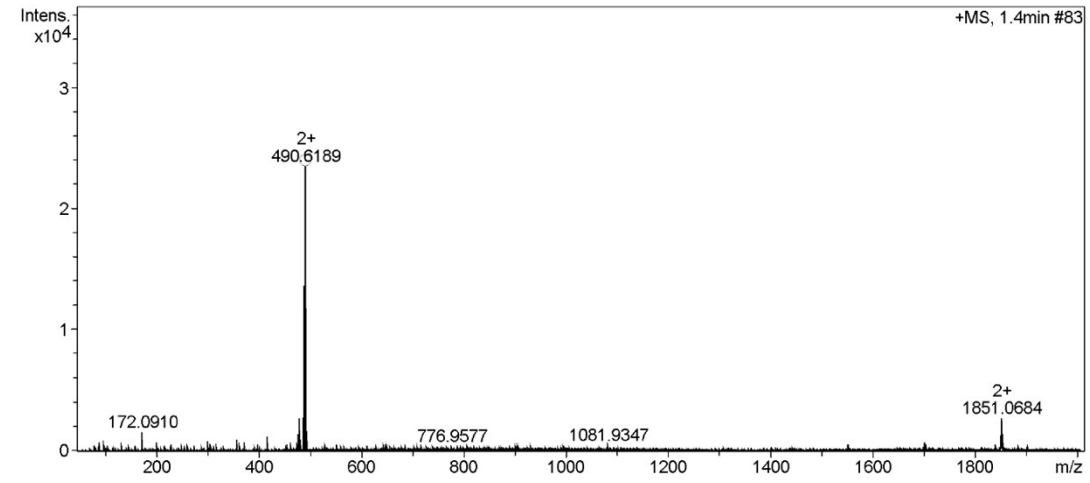

Meas. m/z	#	Ion Formula	m/z	err [mDa]	err [ppm]	rdb	N-Rule	e⁻ Conf	mSigma
490.618879	1	C57H40F3N7Ru	490.617257	1.6	3.3	40.5	-	odd	17.0

Figure S16. ESI HRMS For **Ru3**

5.0 Single Crystal X-Ray Diffraction Data

The X-ray intensity data for **Ru1** and **Ru2** were measured on a Bruker Apex Kappa Duo using a microfocus Copper source (λ = 1.54178 Å). Samples were placed in Cargille NVH immersion oil and mounted on a MiTeGen micromount, cooled and kept at 100K for data collection using an Oxford Cobra Cryosystem low temperature device. See Table S1 for crystal data and structure refinement parameters.

Reflection data were reduced and processed using the Bruker APEX3 suite of programs.[6] Multi-scan absorption corrections were applied using SADABS.[7] The structures were solved using the dual space algorithm XT[8] and refined by full matrix least-squares procedures with XL[9] within the OLEX2 suite.[10] All non-hydrogen atoms were refined with anisotropic displacement parameters. All carbon bound hydrogen atoms were placed in calculated positions and refined with a riding model, with isotropic displacement parameters equal to either 1.2 or 1.5 times the isotropic equivalent of their carrier atoms.

Specific refinement strategies are outlined below and can also be located in the crystallographic information files CCDC 2204851_2204852.

Ru 1: Very weak diffraction, especially at higher angles using LT and long exposures. The diffraction limit was generously set to d = 0.86 for the experiment (2 theta = 128 degrees). The data is also rotationally twinned around 2-axis (1, 0, -1)[3, 0, -2], Angle () [] = 4.24 ® with a twin matrix (0.242, 0.126, -0.758, 0.000, -1.000, 0.000, -1.242, -0.126, -0.242) and a refined BASF 0.354(6). The twin relationship was identified using PLATON, and the weight was adjusted manually. One phenyl ring (C57) on the amine in complex Ru1 was disordered over two locations (71:29% occupancy) and modelled using geometric (SADI, FLAT) and displacement (SIMU) restraints. The CF3 group of Complex Ru1 was also disordered in two locations (69:31% occupancy) and modelled with geometric (DFIX) and displacement (SIMU, ISOR) restraints. Aromatic rings in the complexes near the high residuals were modelled using rigid groups (AFIX 66) and displacement restraints (ISOR). All PF6 anions were modelled with rigid groups and restraints (SIMU). There are 4 solvent sites in the ASU consisting of toluene and DCM, all modelled with rigid groups. Toluene C130, 25%, DCM Cl5, 25%; C137, 25%, Cl7, 25%; C143, 25%, Cl9, 25%; Cl1, 25%, Cl3, 50% occupied and modelled using restraints (SIMU, ISOR).

Ru2: Partially occupied solvents were identified in the asymmetric unit. All were modelled with rigid groups. Site unique molecules - toluene; 33% occupied, DCM; 15% occupied. One site was modelled with 3 solvents - 2 toluene, 32 and 29% occupied and DCM 18% occupied. All moieties in this shared site were kept to a total of 75% occupancy. Geometric restraints were employed (SIMU, ISOR) in modelling these partially occupied solvents.

Crystal data and structure refinement for Ru1 and Ru2		
Identification code	**Ru1**	**Ru2**
CCDC No.	2204851	2204852
Empirical formula	$C_{58.38}H_{44.5}Cl_{1.5}F_{15}N_7P_2Ru$	$C_{63.95}H_{48.23}Cl_{0.66}F_{15}N_7P_2Ru$
Formula weight	1345.19	1385.96
Temperature (K)	100(2)	100(2)
Crystal system	triclinic	Monoclinic
Space group	$P\bar{1}$	C2/c
a (Å)	17.5338(13)	18.3727(8)
b (Å)	19.1373(12)	23.3211(10)
c (Å)	20.747(2)	31.2846(12)
α (°)	107.594(6)	90
β (°)	98.679(6)	105.648(2)
γ (°)	109.219(4)	90
V (Å^3)	6018.8(9)	12907.7(9)
Z	4	8
ρ_{calc} (g /cm^3)	1.485	1.426
μ (mm^{-1})	4.026	3.459
F(000)	2713.0	5609.0
Crystal size (mm^3)	0.227 × 0.093 × 0.032	0.219 × 0.034 × 0.031
Radiation	Cu Kα (λ = 1.54178)	Cu Kα (λ = 1.54178)
2Θ range (°)	5.28 to 126.73	5.868 to 128.406
Index ranges	-20 ≤ h ≤ 19, -21 ≤ k ≤ 21, -22 ≤ l ≤ 23	-21 ≤ h ≤ 21, -27 ≤ k ≤ 27, -36 ≤ l ≤ 36
Reflections collected	19160	77737
Independent reflections	19160 R_{int} = 0.1178, R_{sigma} = 0.1110	10736 R_{int} = 0.1171, R_{sigma} = 0.0878
Data/restraints/parameters	19160/873/1624	10736/427/937
Goodness-of-fit on F^2	1.093	1.036
Final R indexes [I≥2σ (I)]	R_1 = 0.1491, wR_2 = 0.4506	R_1 = 0.0901, wR_2 = 0.2511
Final R indexes [all data]	R_1 = 0.1824, wR_2 = 0.4999	R_1 = 0.1326, wR_2 = 0.2935
Largest diff. peak/hole (e Å^{-3})	4.72/-1.80	2.11/-0.69

Table S1. Crystal data and structure refinement for **Ru1** and **Ru2**.

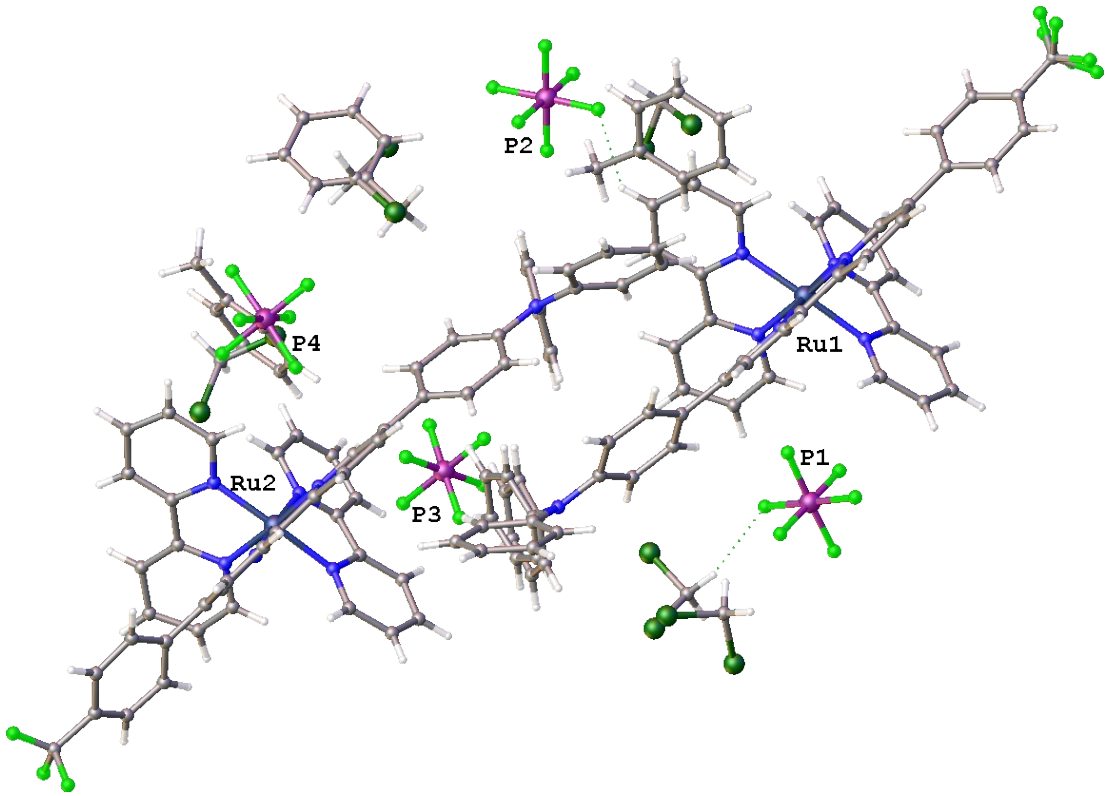

Figure S17. Disordered molecular structure of **Ru1**, with partially occupied disordered solvent (toluene/DCM) sites. Selected atoms labelled for clarity.

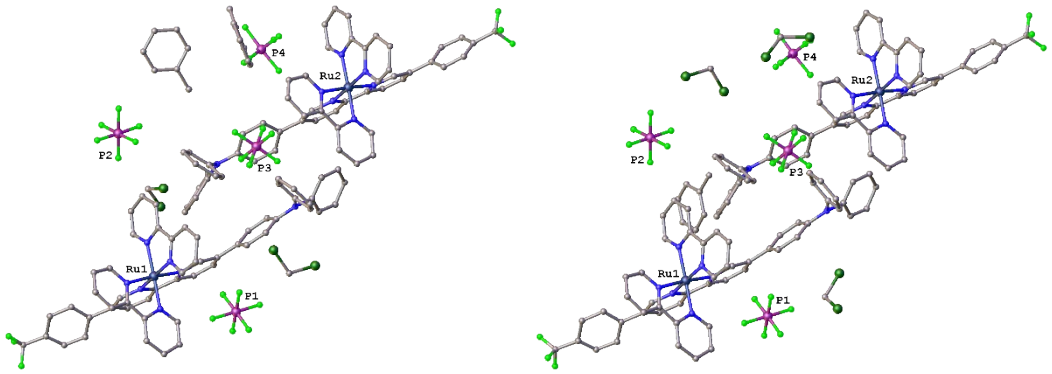

Figure S18. Individual representations of each disordered moiety in **Ru1** with (left) the majority occupied moiety (phenyl/CF_3 71 and 69%, toluene 0.25% occupied and CH_2Cl_2, 50% occupied) and (right) minor occupied moiety (phenyl/CF_3 29 and 31%, toluene 0.25% occupied and CH_2Cl_2, 25% occupied).

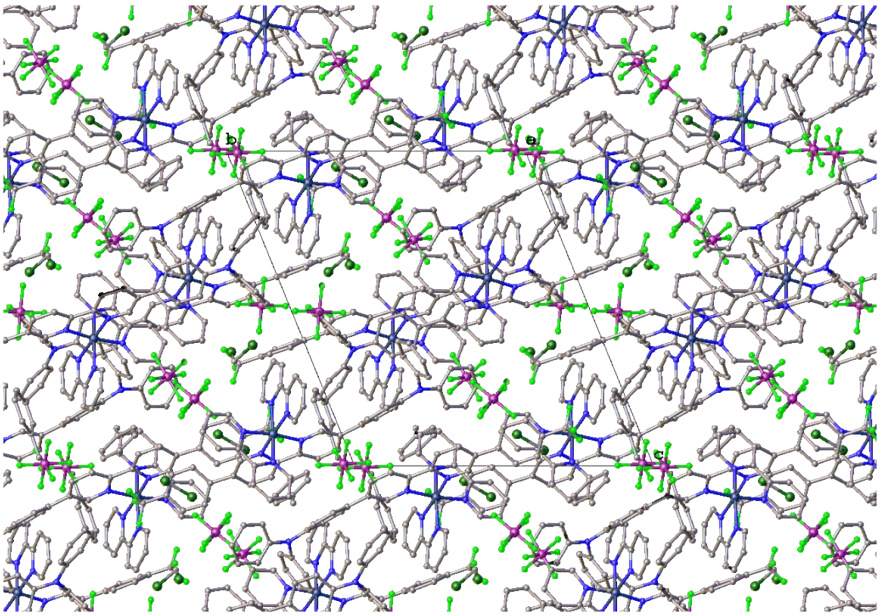

Figure S19. Schematic packing diagram of the major occupied moieties in **Ru1** only viewed normal to the a-axis, with hydrogen atoms omitted for clarity

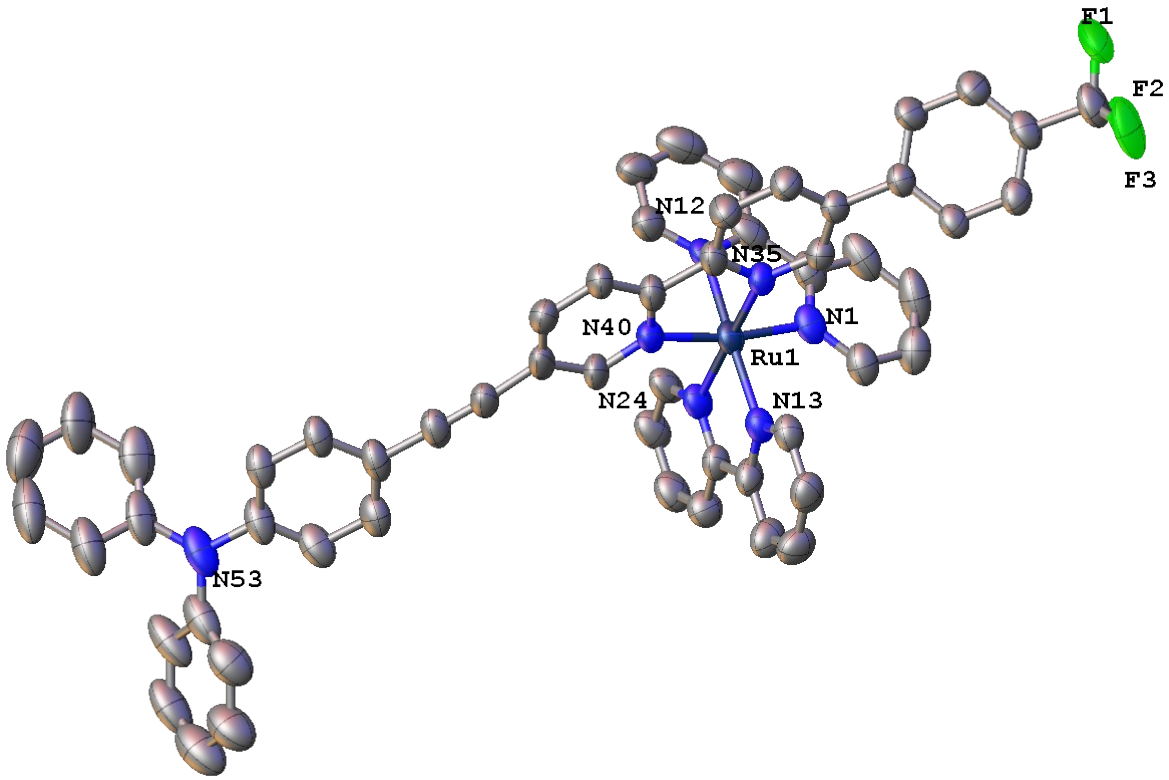

Figure S20. Structure of **Ru2** with atomic displacement shown at 50% occupancy. Hydrogen atoms omitted for clarity. Heretoatoms labelled only

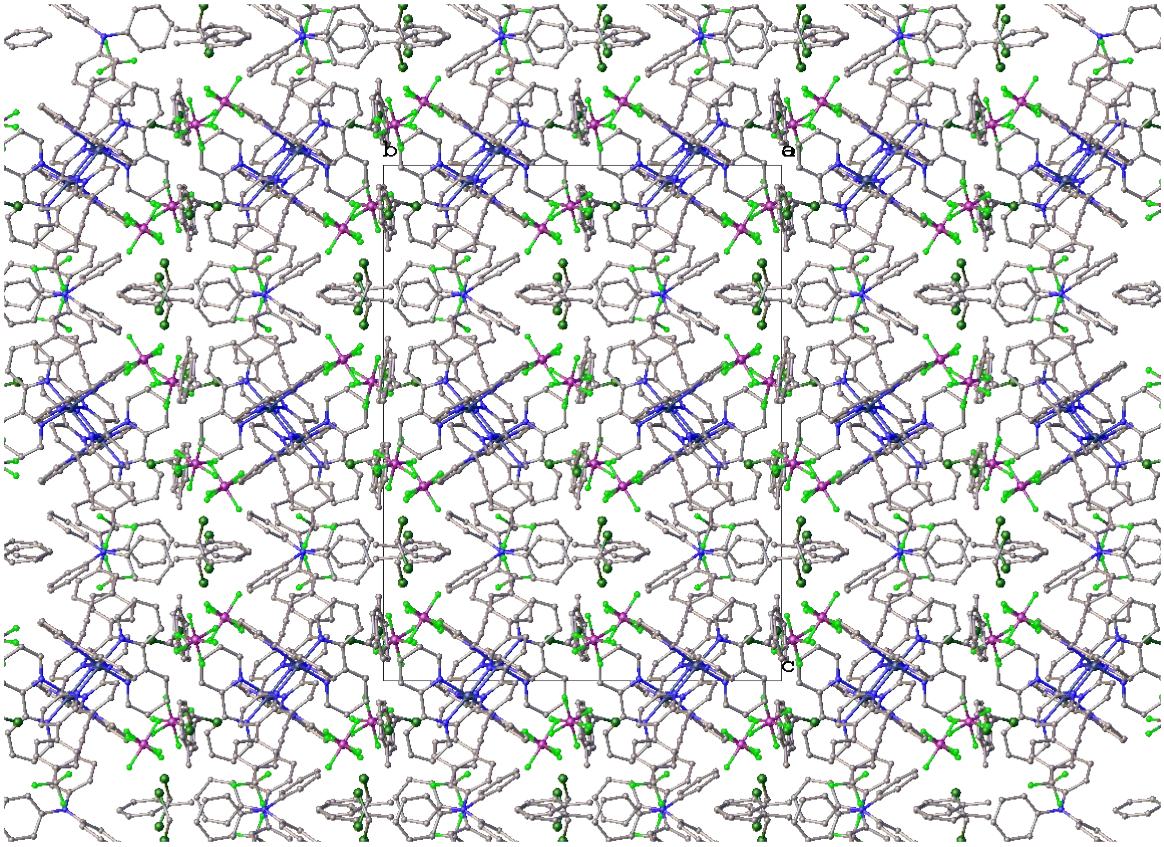

Figure S21. Schematic packing diagram of **Ru2** shown normal to the a-axis . Hydrogen atoms omitted for visual clarity.

6.0 Photophysical Measurements

6.1 Solvatochromism Studies L1-3

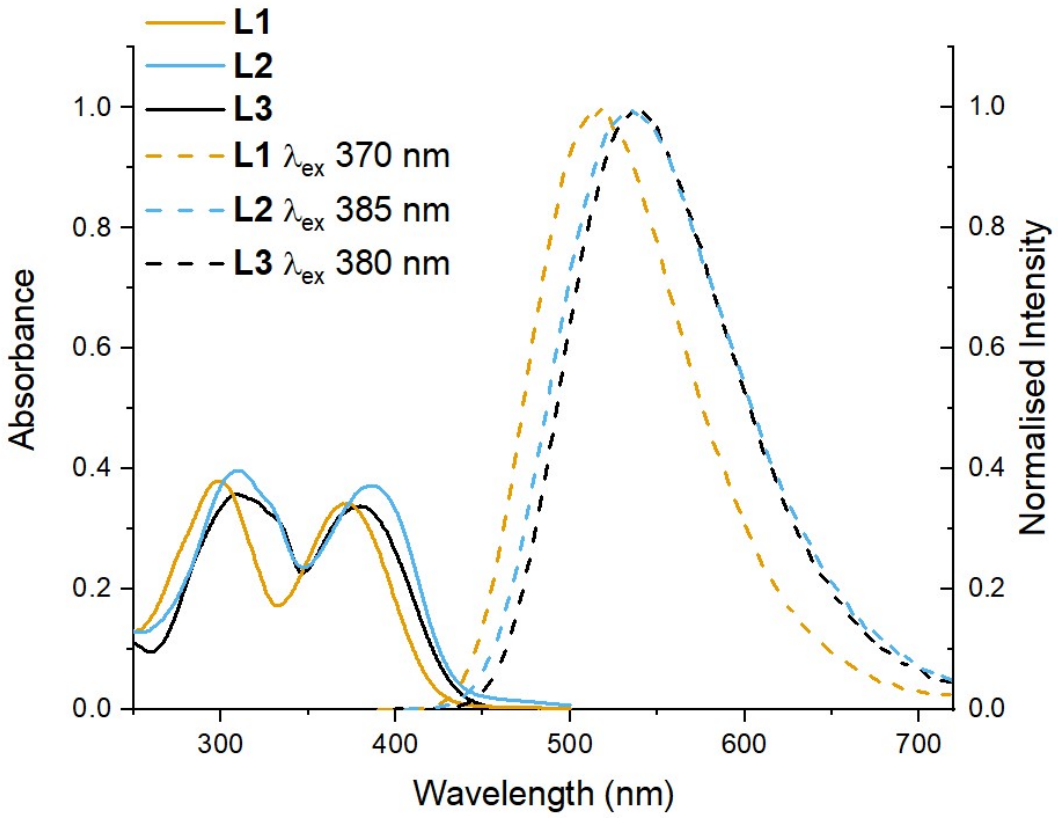

Figure S22. Absorption (solid lines) and emission (dashed lines) spectra of **L1ac** (orange), **L2ad** (blue) and **L3bc** (black). CH_2Cl_2 [10^{-5} M], 298 K.

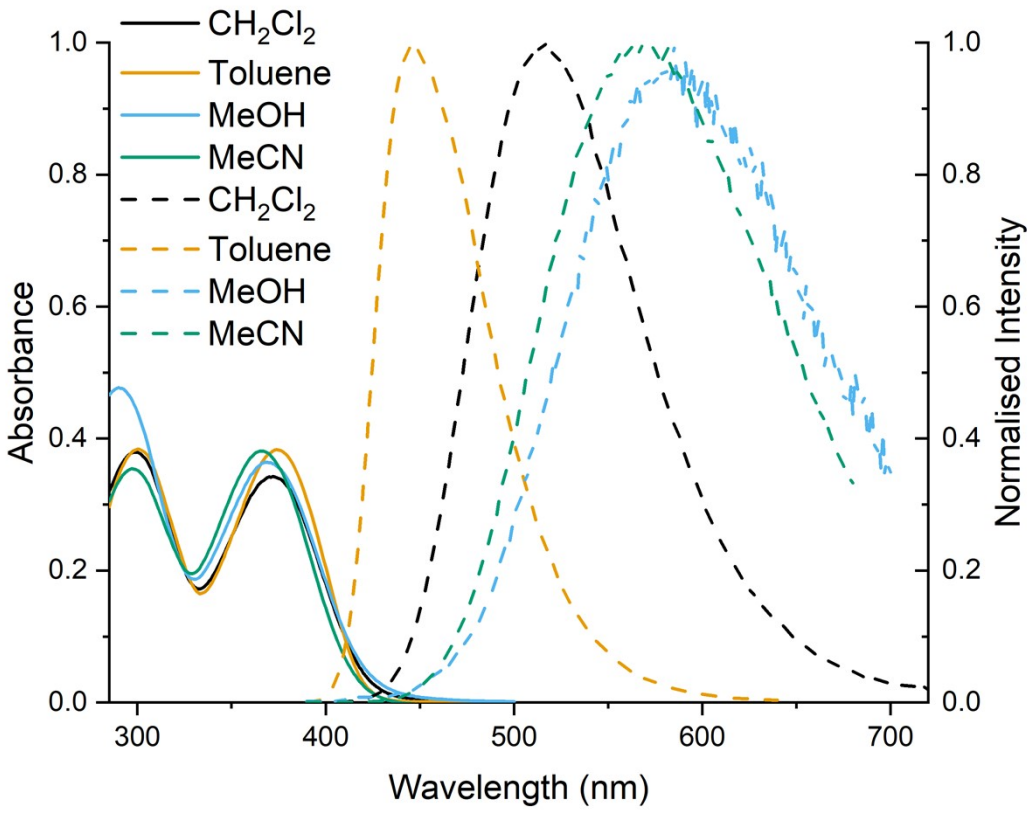

Figure S23. Solvatochromic studies of **L1ab** in CH_2Cl_2, MeCN, Toluene and MeOH; UV-vis spectra shown with solid lines and normalised emission spectra shown with dotted lines (λ_{ex} = 370 nm), [10^{-5} M], 298 K

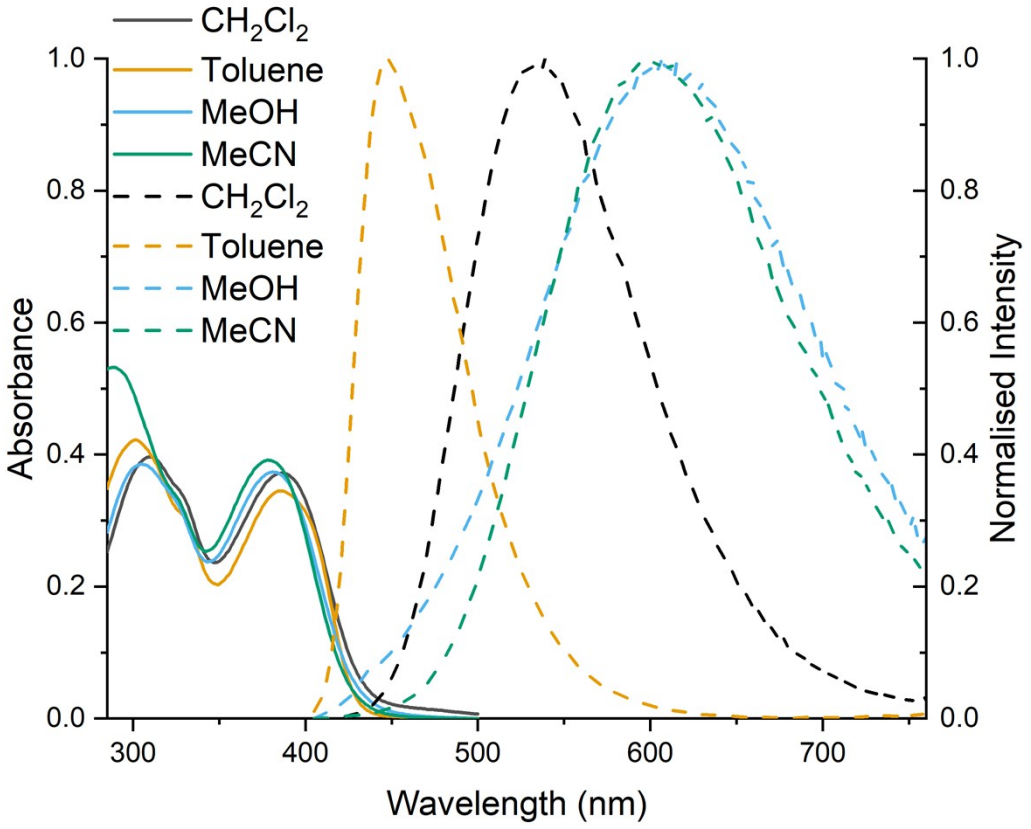

Figure S24. Solvatochromic studies of **L2ad** in CH_2Cl_2, MeCN, Toluene and MeOH; UV-vis spectra shown with solid lines and normalised emission spectra shown with dotted lines (λ_{ex} = 385 nm), [10^{-5} M], 298 K

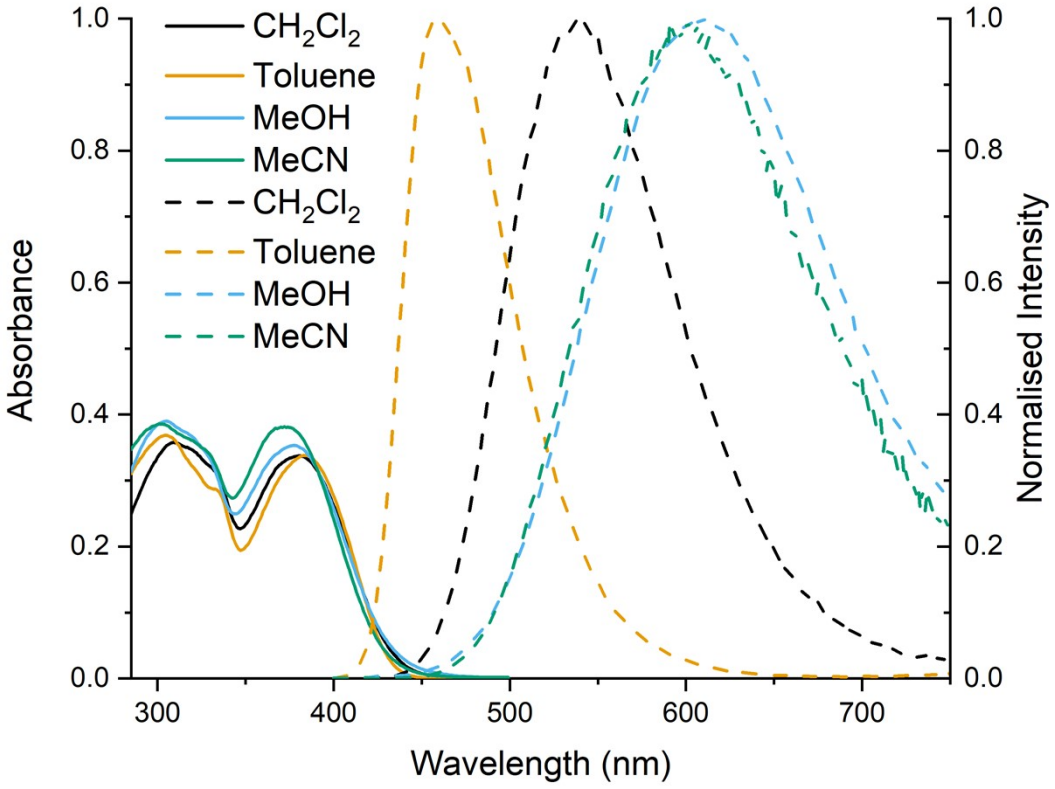

Figure S25. Solvatochromic studies of **L3bc** in CH_2Cl_2, MeCN, Toluene and MeOH; UV-vis spectra shown with solid lines and normalised emission spectra shown with dotted lines (λ_{ex} = 380 nm), [10^{-5} M], 298 K

6.2 Concentration Studies **L1-3**

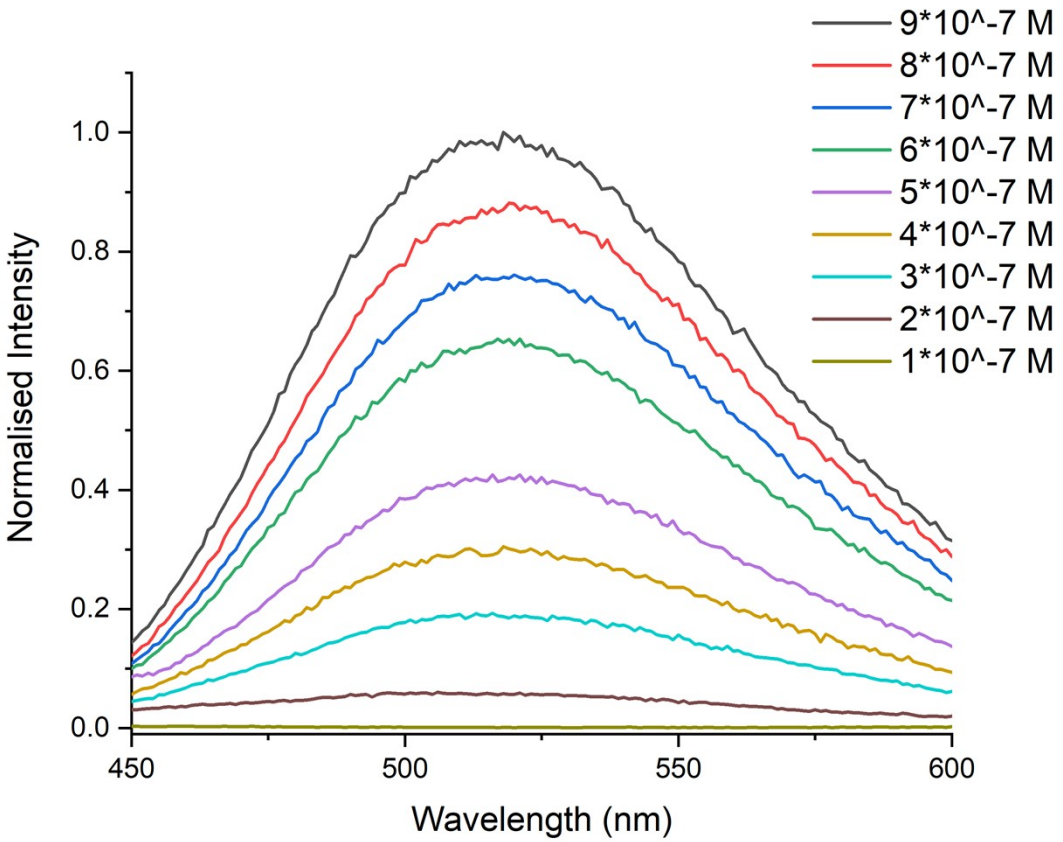

Figure S26. Concentration studies of **L1ac** in CH_2Cl_2 at 298 K

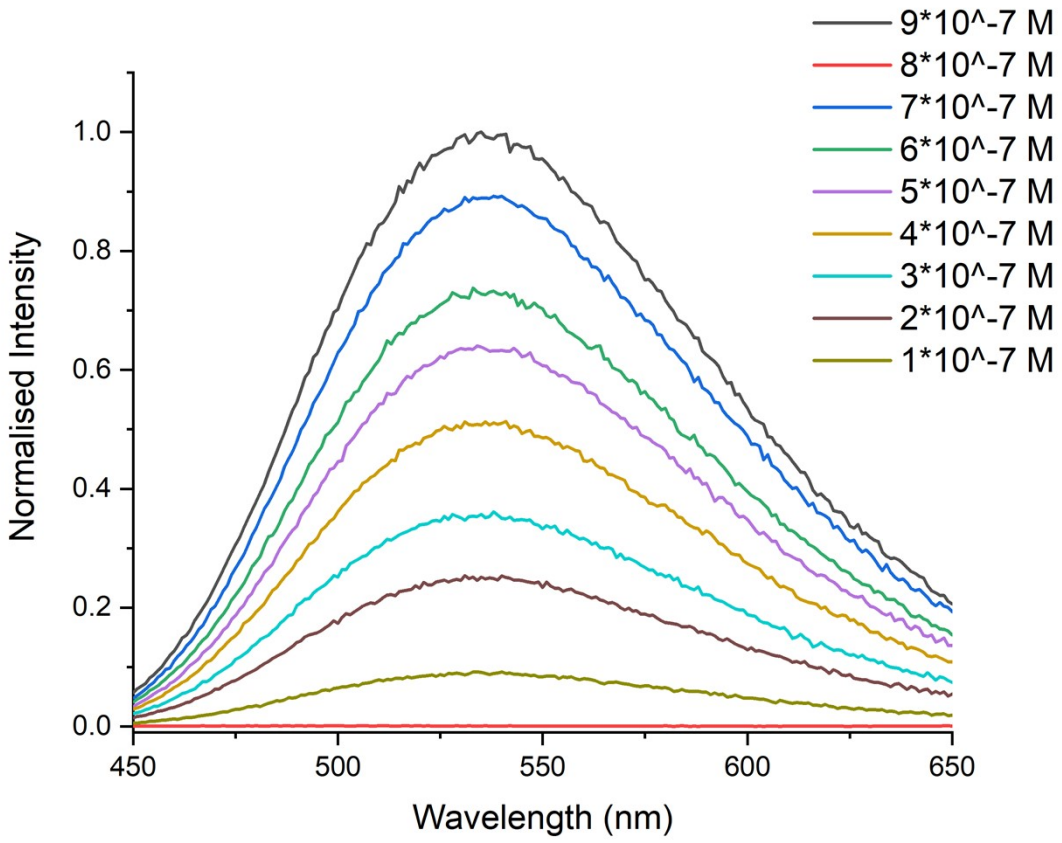

Figure S27. Concentration studies of **L2ad** in CH_2Cl_2 at 298 K

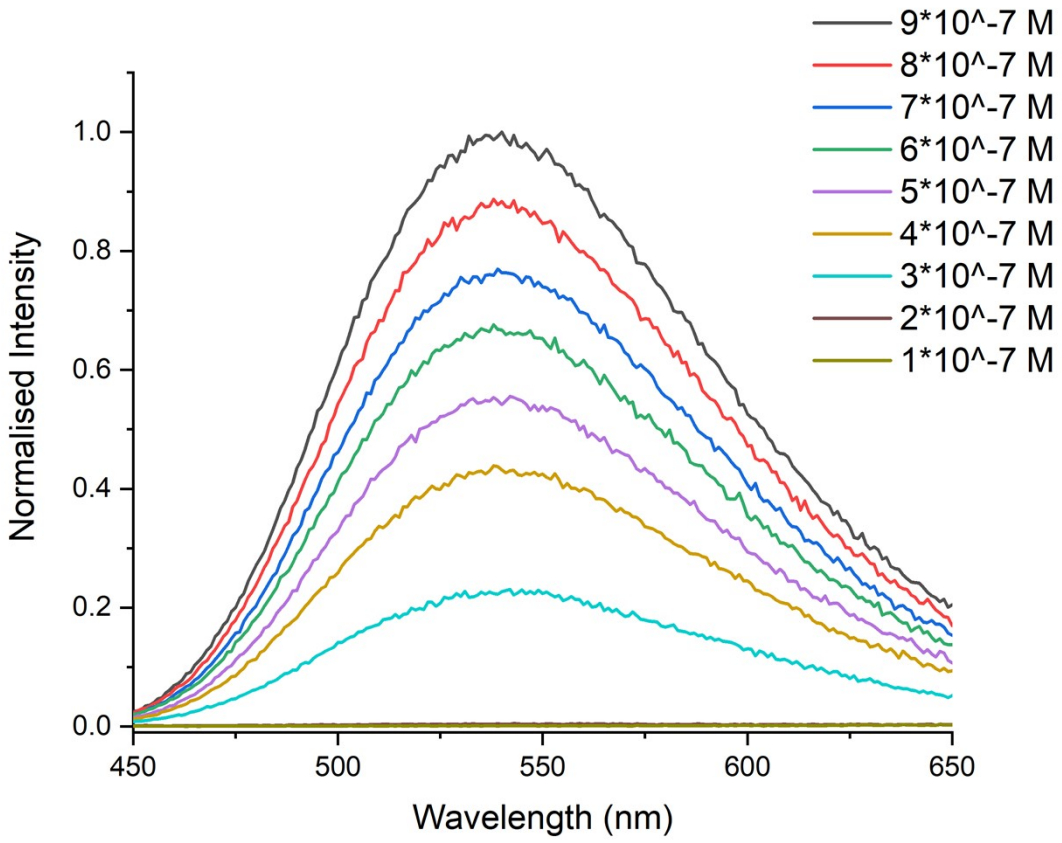

Figure S28. Concentration studies of **L3bc** in CH_2Cl_2 at 298 K

6.3 Low Temperature Emission Studies **L1-3**

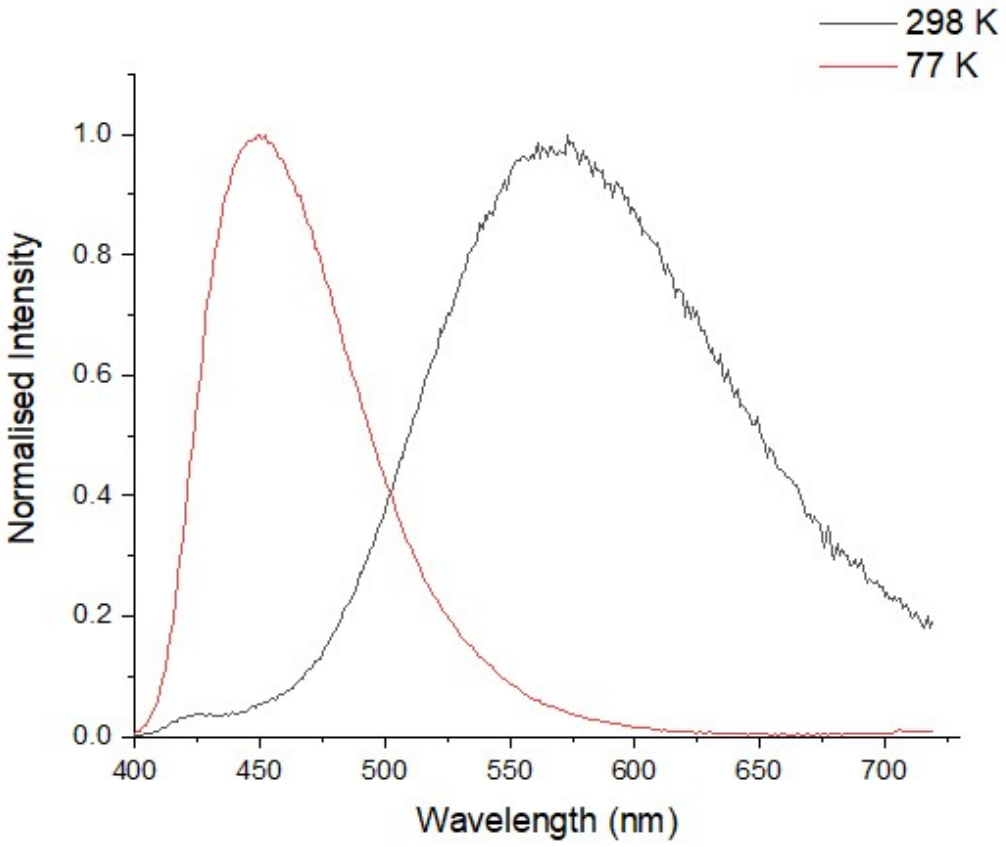

Figure S29. Emission spectra of **L1ac** (λ_{ex} = 375 nm) at 298 K (red line) and 77 k (black line) in 4:1 EtOH:MeOH

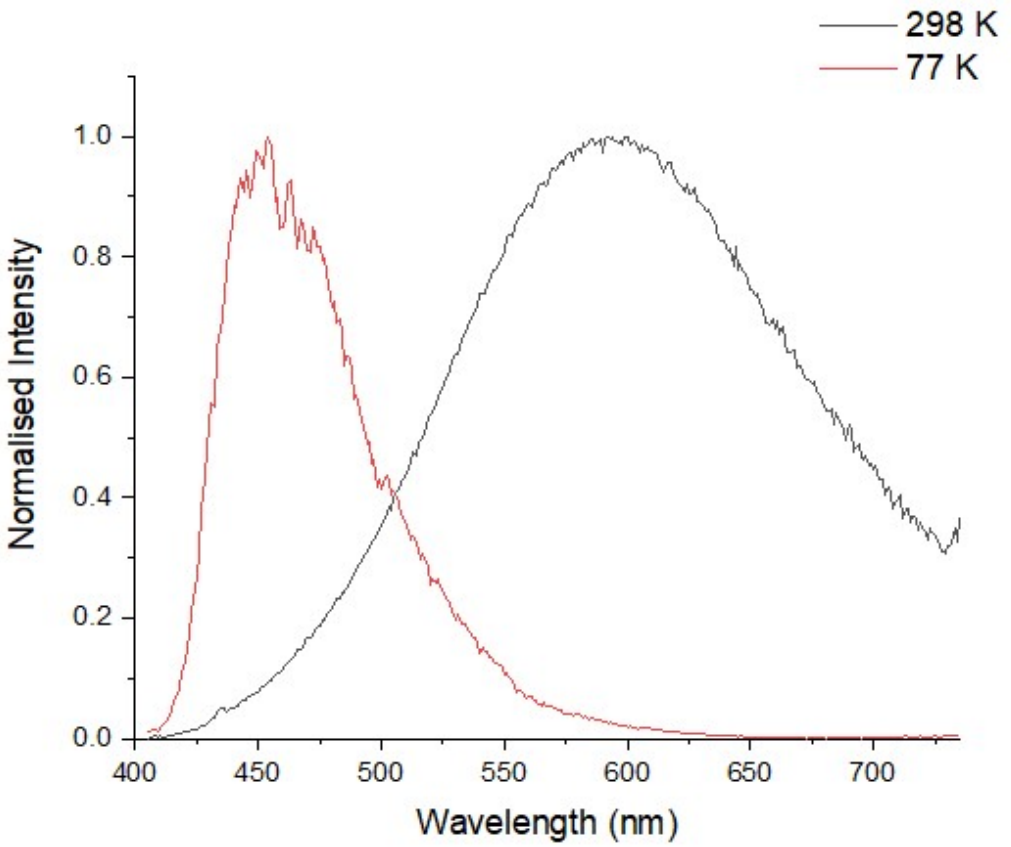

Figure S30. Emission spectra of **L2ad** (λ_{ex} = 390 nm) at 298 K (red line) and 77 k (black line) in 4:1 EtOH:MeOH

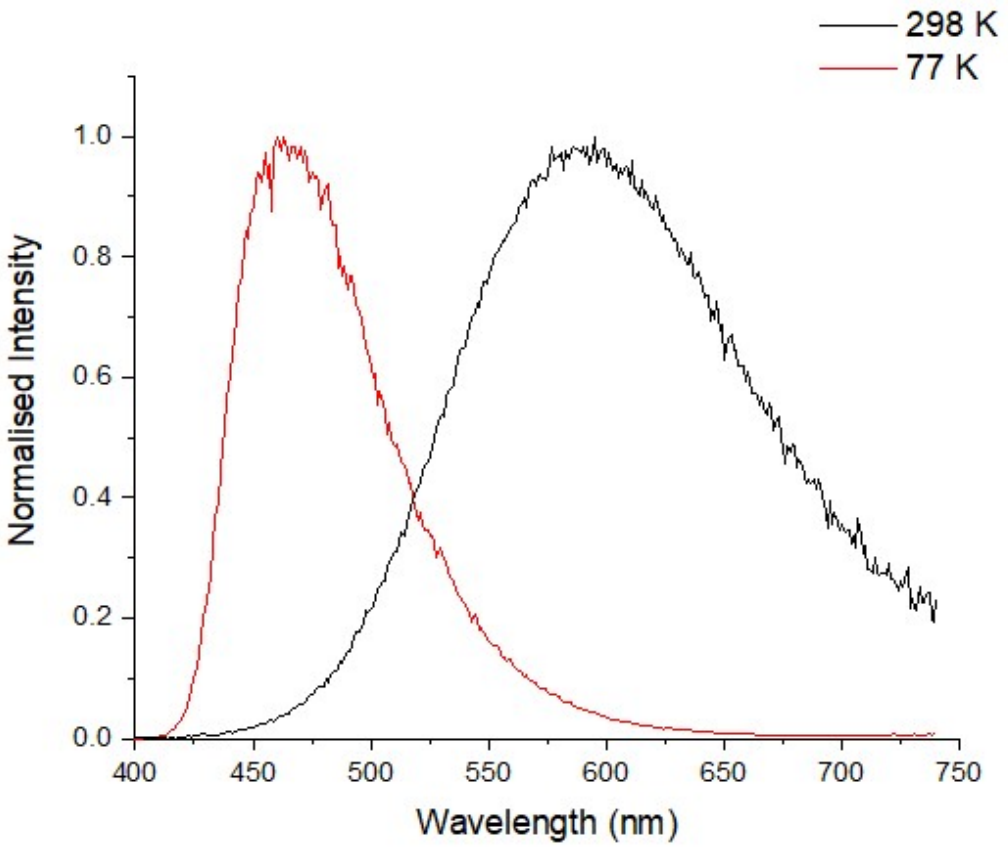

Figure S31. Emission spectra of **L3bc** (λ_{ex} = 380 nm) at 298 K (red line) and 77 k (black line) in 4:1 EtOH:MeOH

6.4 Solvatochrimism Studies **Ru1-3**

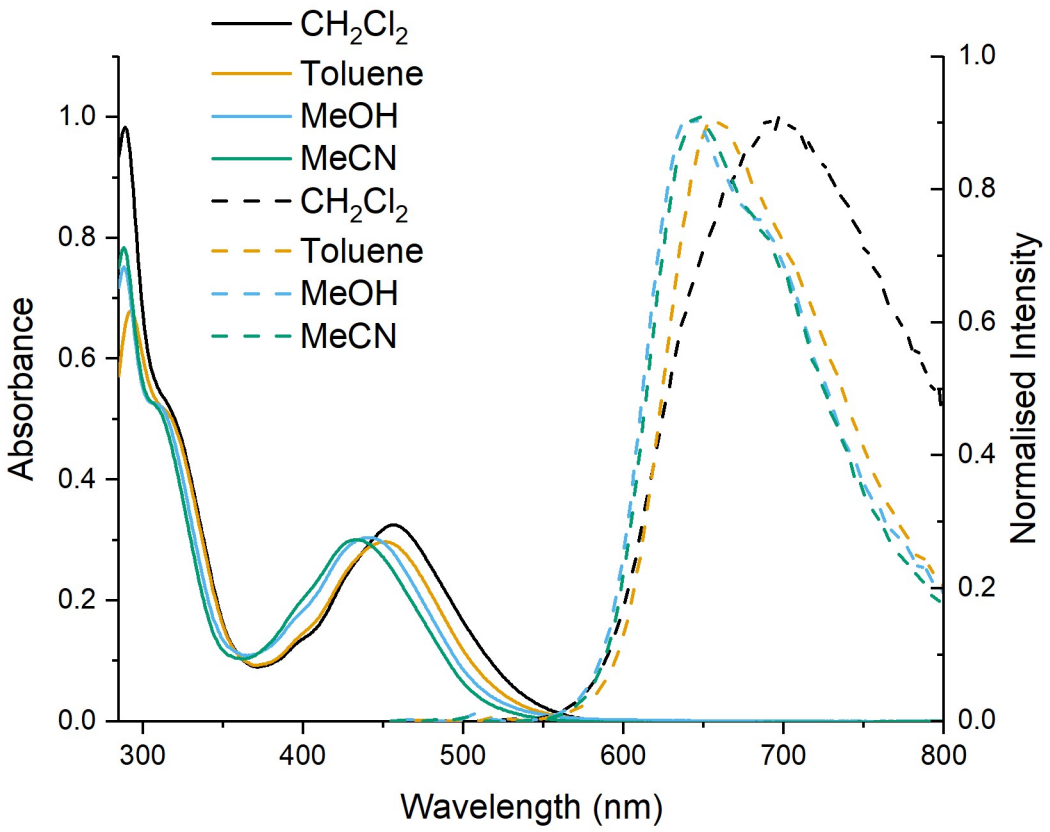

Figure S32. Solvatochromic studies of **Ru1** in CH_2Cl_2, MeCN, Toluene and MeOH; UV-vis spectra shown with solid lines and normalised emission spectra shown with dotted lines (λ_{ex} was absorption max), [10^{-5} M], 298 K

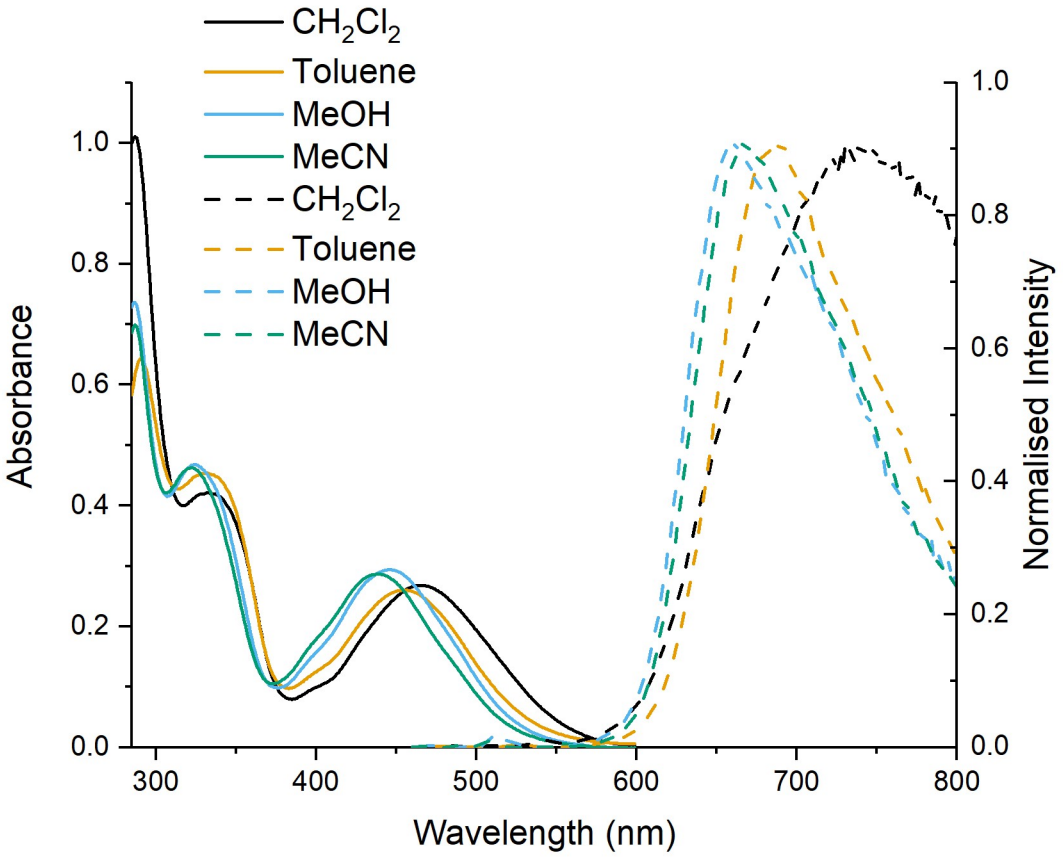

Figure S33. Solvatochromic studies of **Ru2** in CH_2Cl_2, MeCN, Toluene and MeOH; UV-vis spectra shown with solid lines and normalised emission spectra shown with dotted lines (λ_{ex} was absorption max in given solvent), [10^{-5} M], 298 K

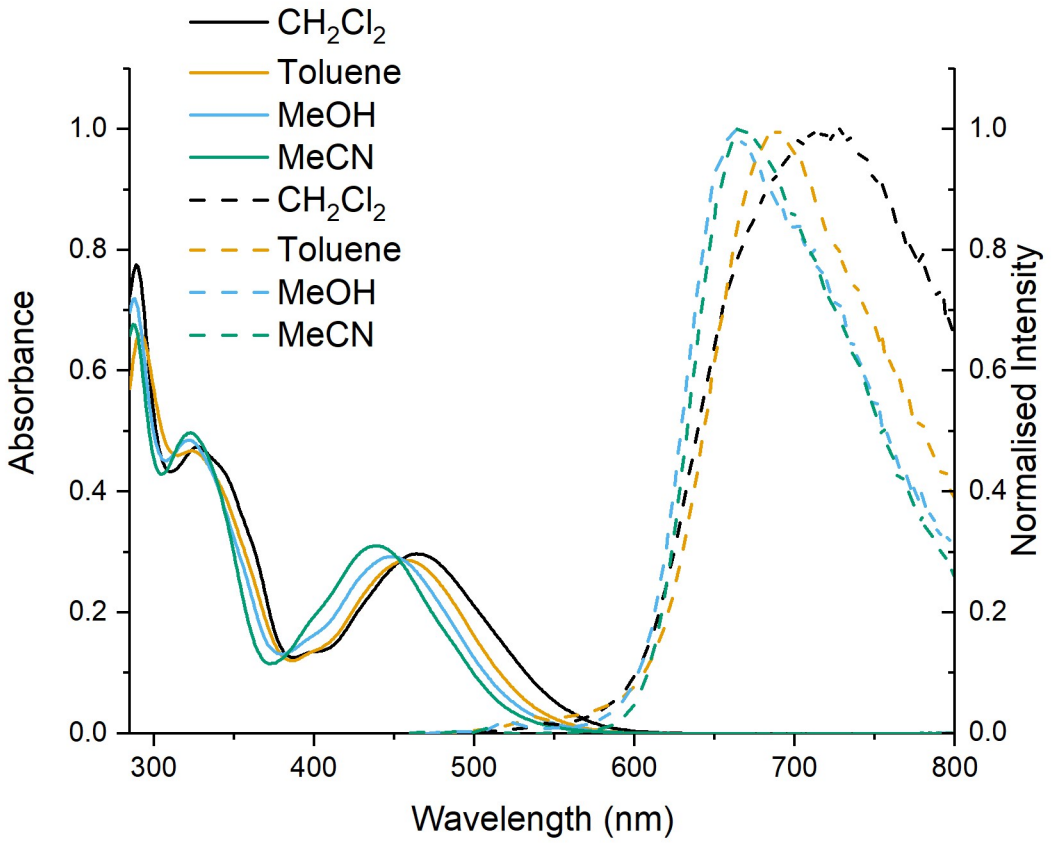

Figure S34. Solvatochromic studies of **Ru3** in CH_2Cl_2, MeCN, Toluene and MeOH; UV-vis spectra shown with solid lines and normalised emission spectra shown with dotted lines (λ_{ex} was absorption max in given solvent), [10^{-5} M], 298 K

6.5 Excitation Spectra of **Ru1-3** in MeCN and CH_2Cl_2

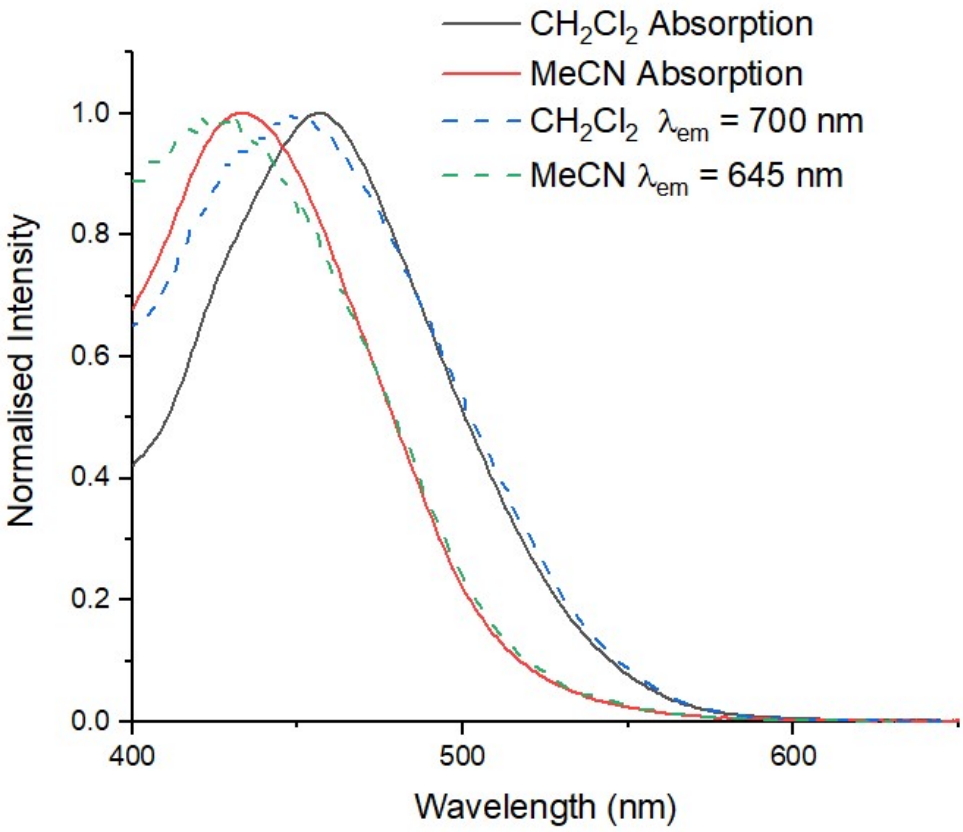

Figure S35. Excitation studies of **Ru1** in MeCN and CH_2Cl_2 (dashed lines), λ_{ex} = 435 nm for MeCN, 460 nm for CH_2Cl_2), [10^{-5} M], 298 K compared to absorption profiles of **Ru1** in MeCN and CH_2Cl_2 (solid lines) [10^{-5} M], 298 K

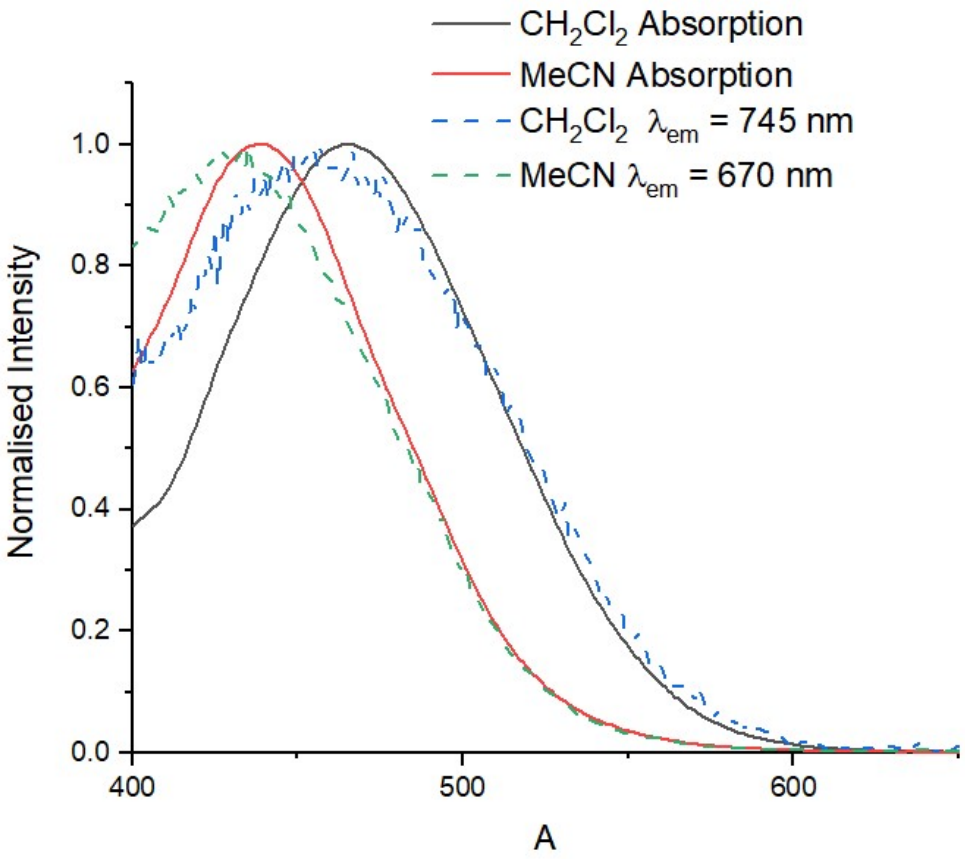

Figure S36. Excitation studies of **Ru2** in MeCN and CH_2Cl_2 (dashed lines), λ_{ex} = 440 nm for MeCN, 465 nm for CH_2Cl_2), [10^{-5} M], 298 K compared to absorption profiles of Ru1 in MeCN and CH_2Cl_2 (solid lines) [10^{-5} M], 298 K

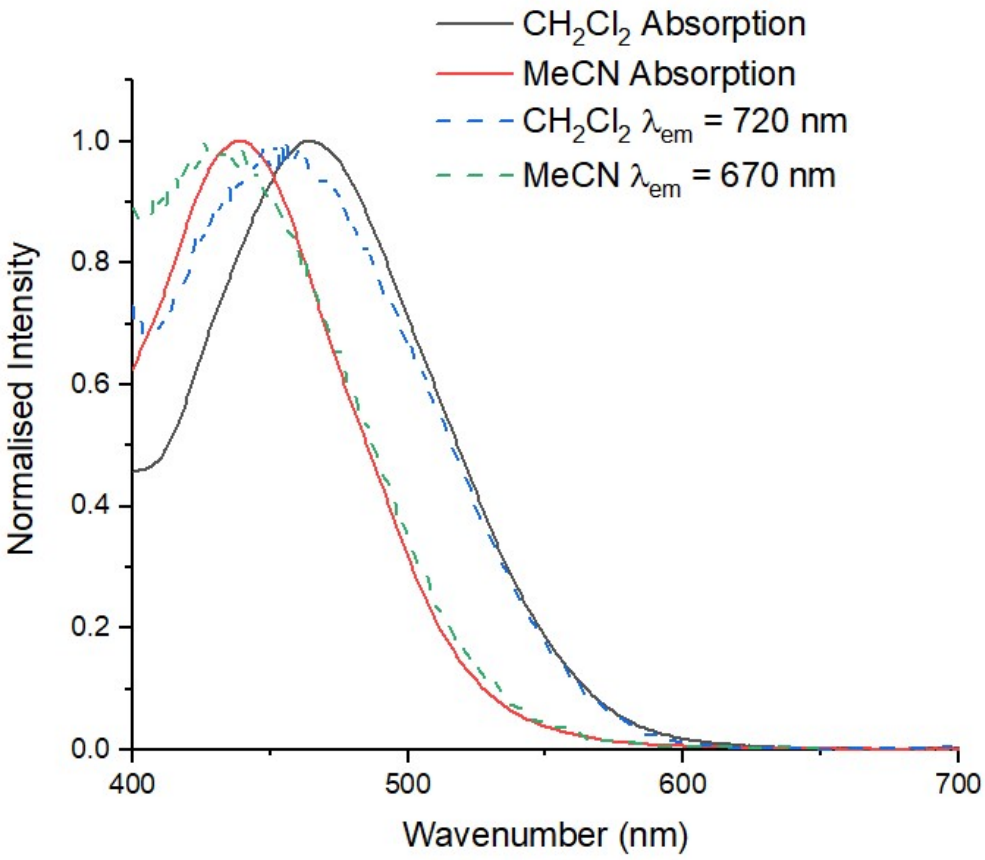

Figure S37. Excitation studies of **Ru3** in MeCN and CH_2Cl_2 (dashed lines), λ_{ex} = 440 nm for MeCN, 465 nm for CH_2Cl_2), [10^{-5} M], 298 K compared to absorption profiles of **Ru1** in MeCN and CH_2Cl_2 (solid lines) [10^{-5} M], 298 K

6.6 Lifetime Traces

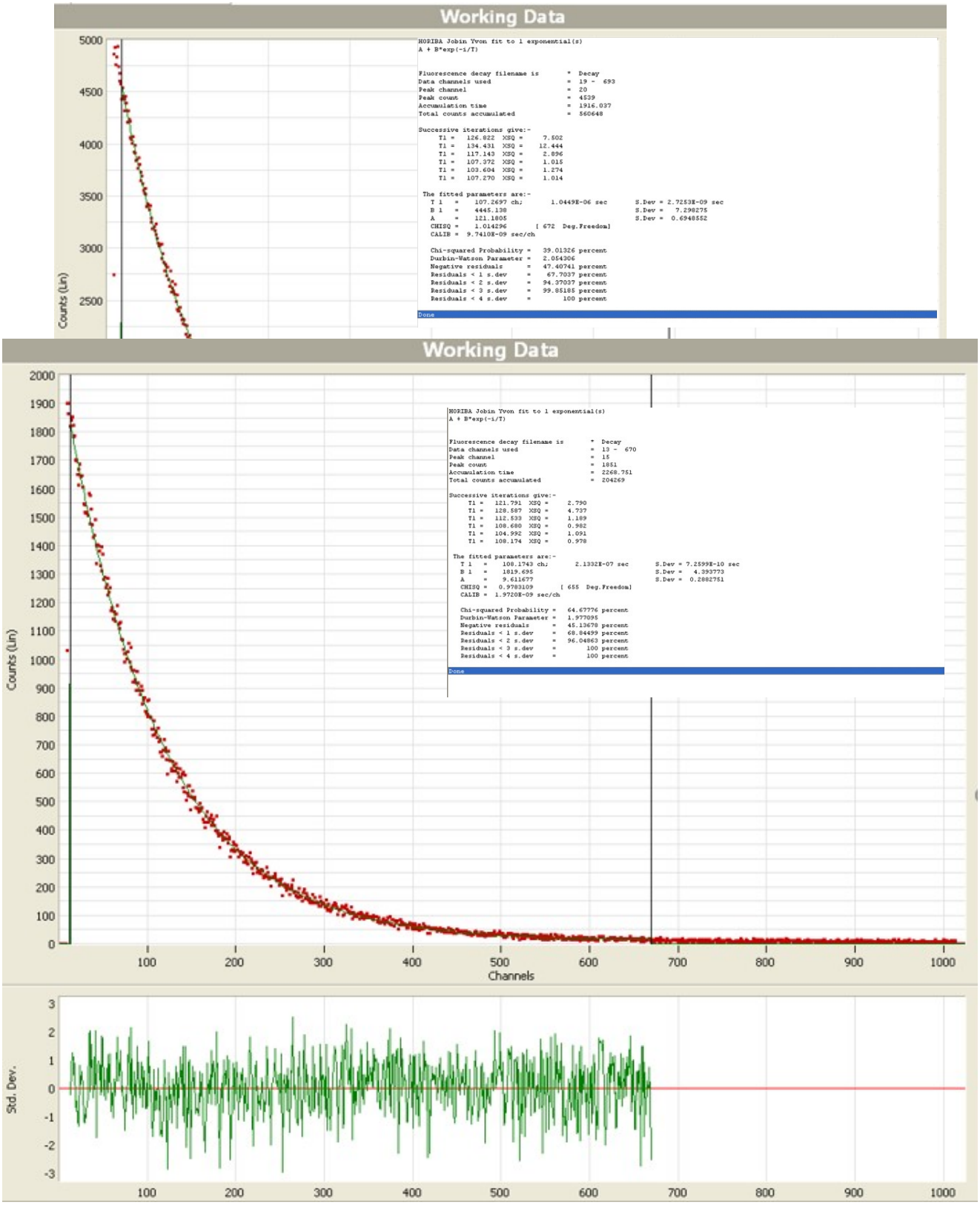

Figure S39. Emission lifetime decay trace of **Ru2** (λ_{ex} = 460 nm, $\lambda_{detection}$ = 640 nm) in deaerated MeCN. Fitted with a monoexponential equation CHISQ = 0.978; Durbin-Watson parameter = 1.977.

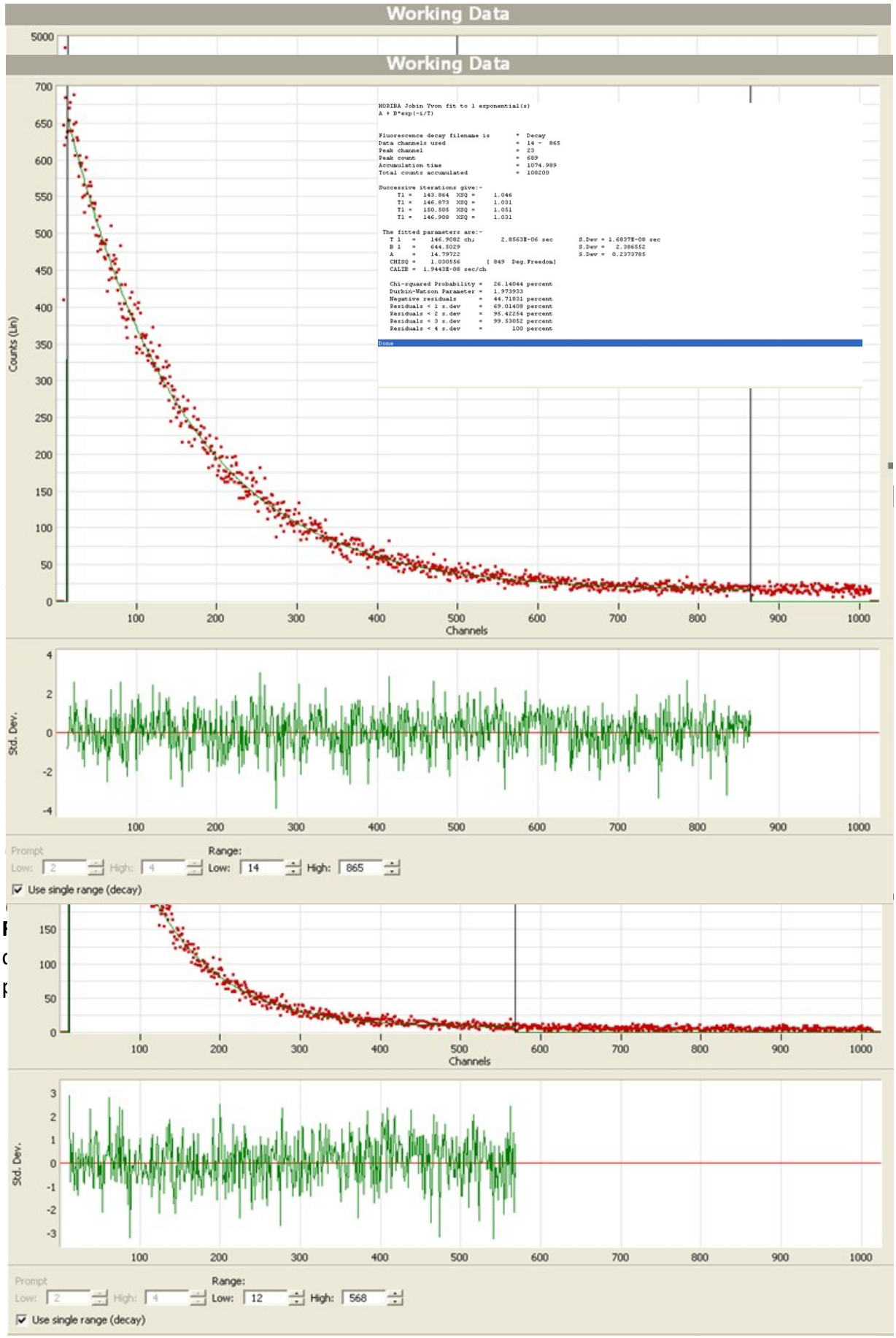

Figure S42. Emission lifetime decay trace of **Ru2** (λ_{ex} = 460 nm, $\lambda_{detection}$ = 720 nm) in deaerated CH_2Cl_2. Fitted with a monoexponential equation CHISQ = 0.985; Durbin-Watson

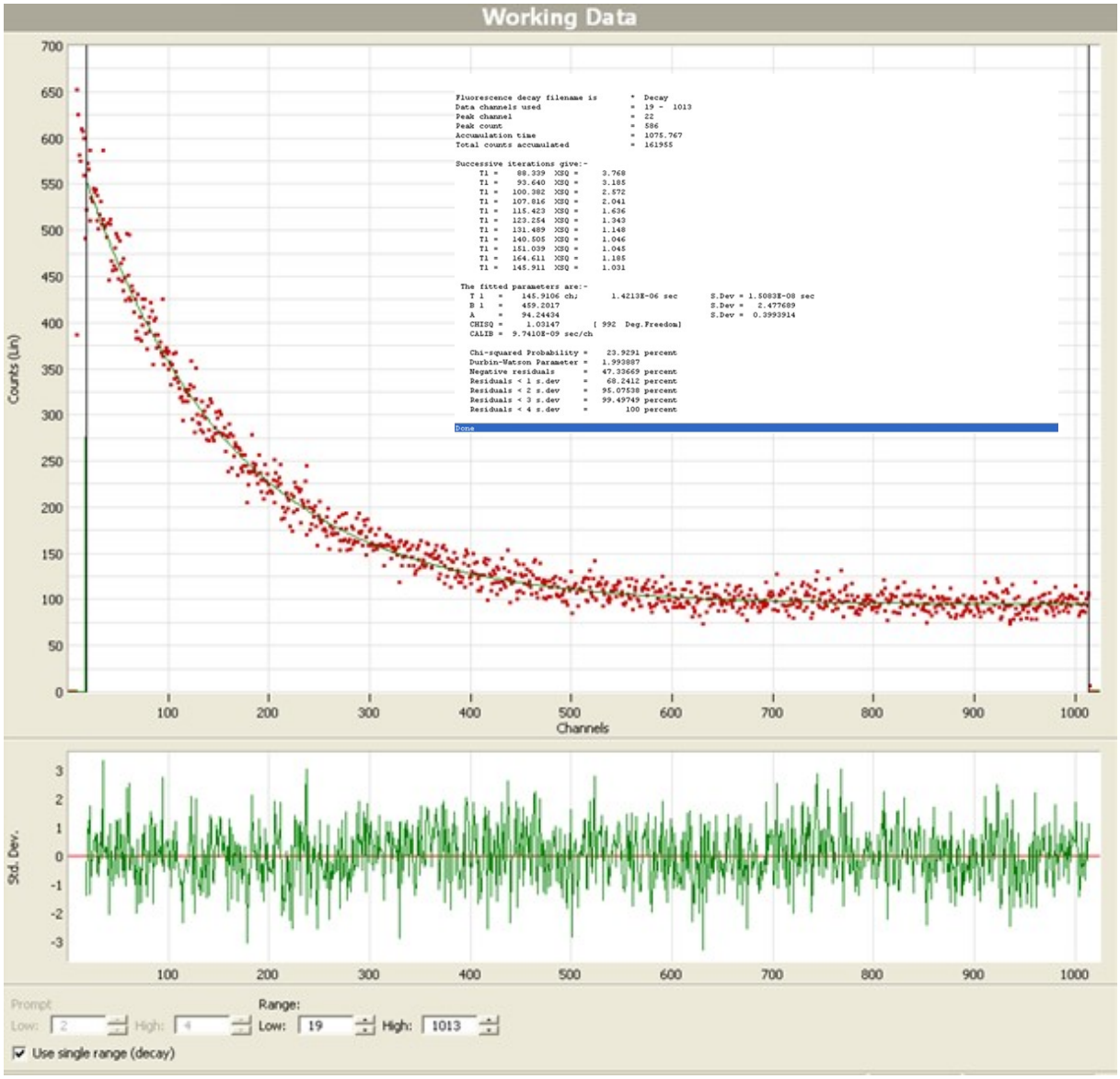

Figure S43. Emission lifetime decay trace of **Ru3** (λ_{ex} = 460 nm, $\lambda_{detection}$ = 720 nm) in deaerated CH_2Cl_2. Fitted with a monoexponential equation CHISQ = 1.031; Durbin-Watson parameter = 1.993.

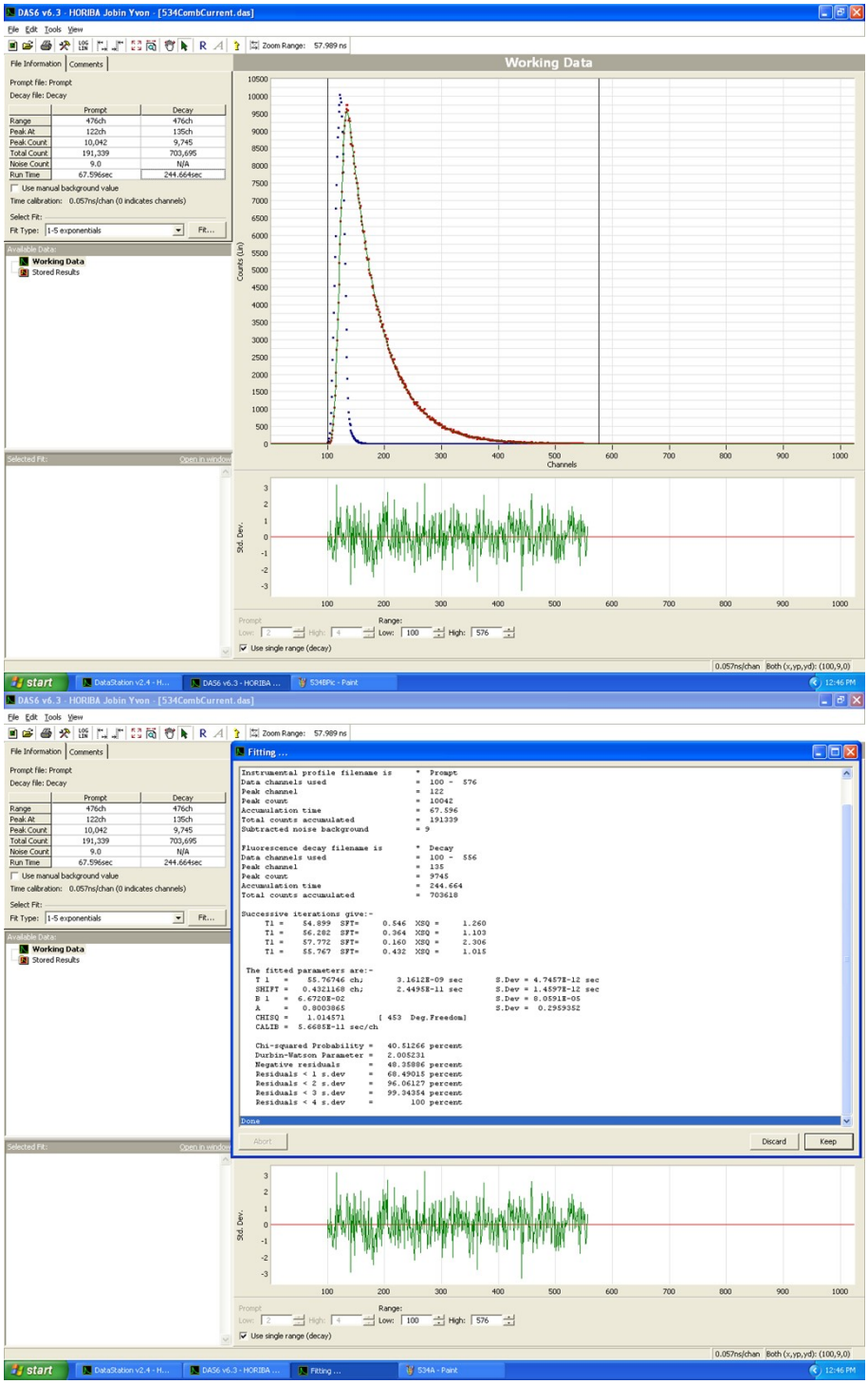

Figure S44. Emission lifetime decay trace of **L1ac** (λ_{ex} = 372 nm, $\lambda_{detection}$ = 520 nm) in CH_2Cl_2. Fitted with a monoexponential equation CHISQ = 1.014; Durbin-Watson parameter = 2.005.

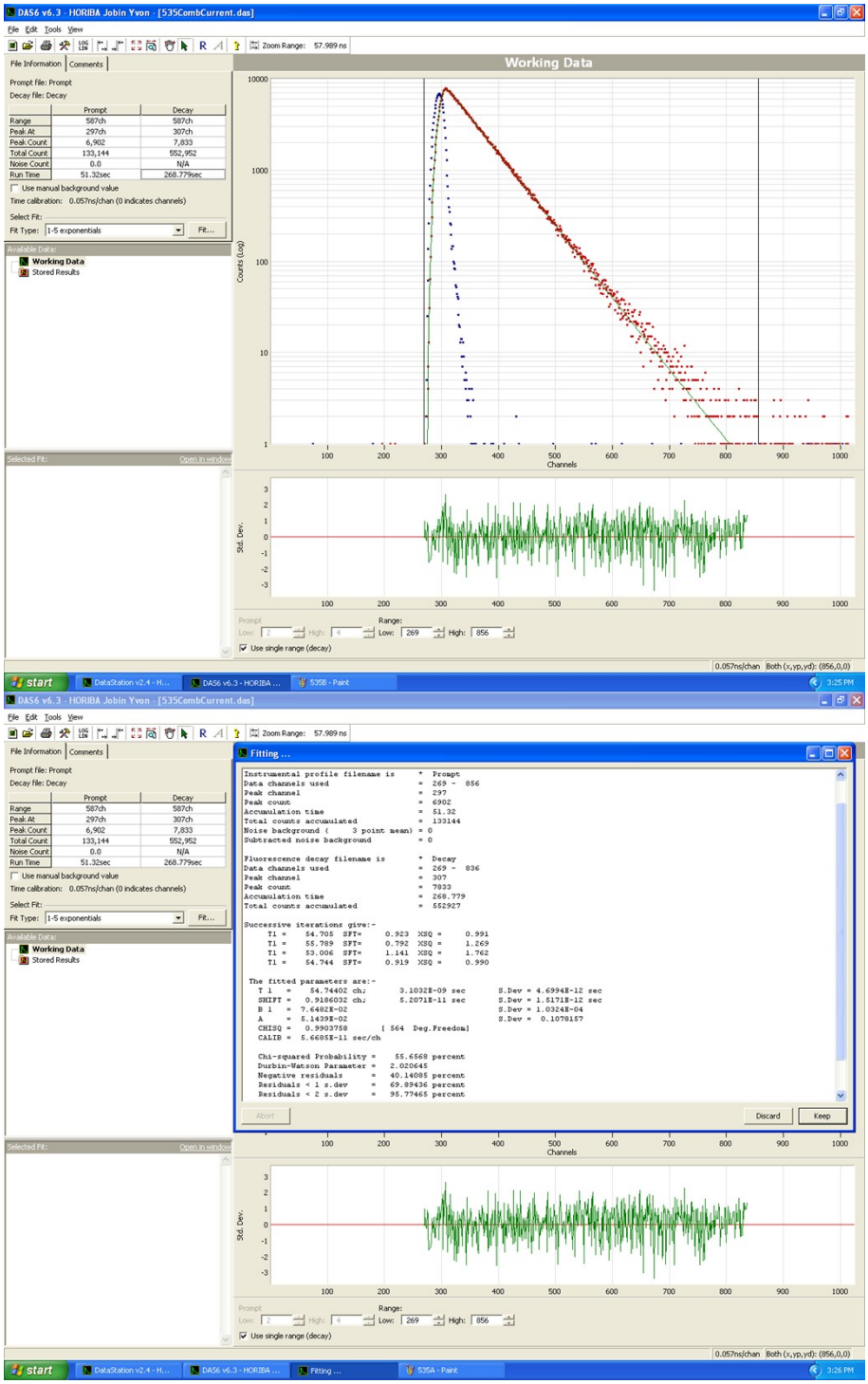

Figure S45. Emission lifetime decay trace of **L2ad** (λ_{ex} = 372 nm, $\lambda_{detection}$ = 540 nm) in CH_2Cl_2. Fitted with a monoexponential equation CHISQ = 0.9904; Durbin-Watson parameter = 2.021

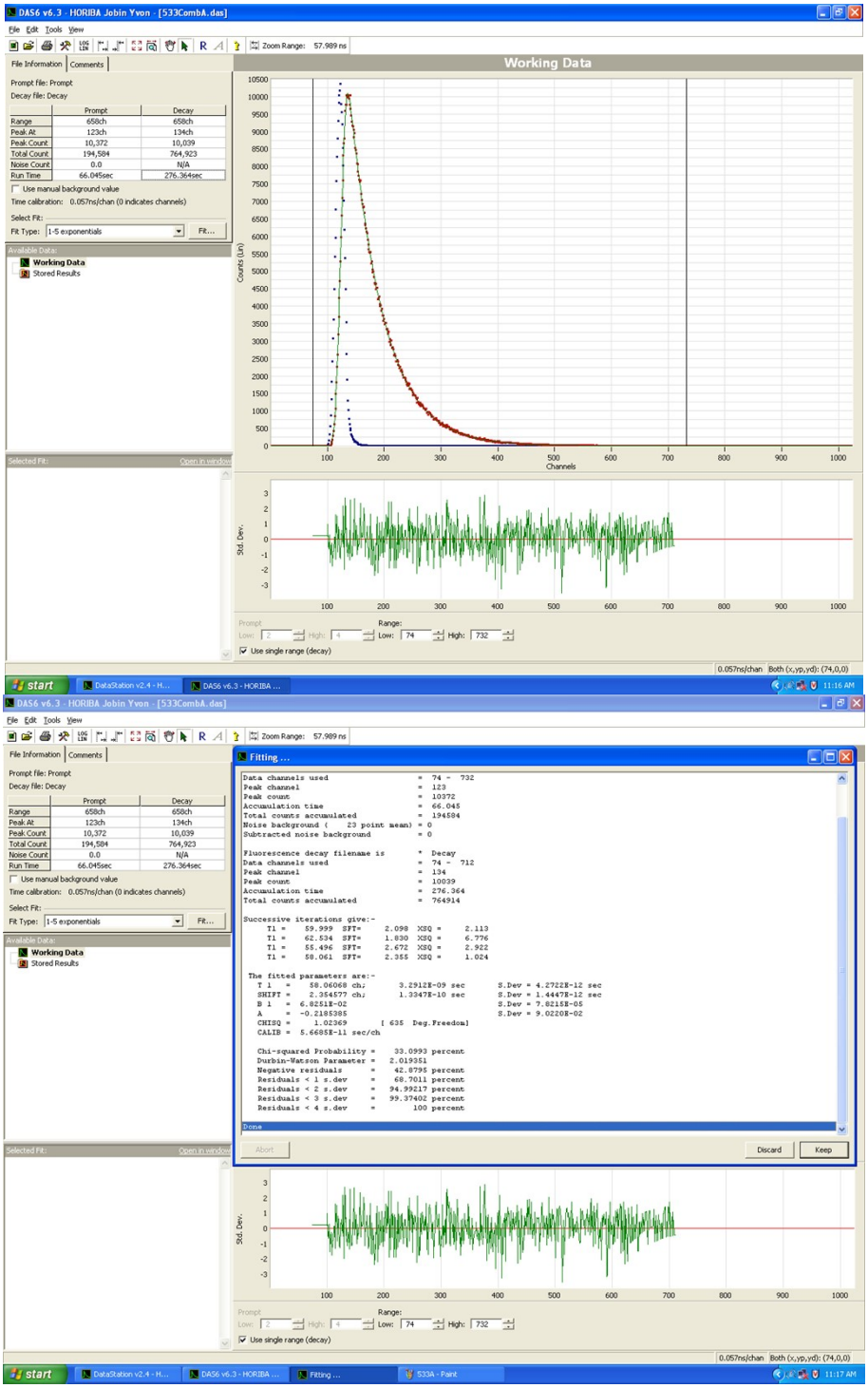

Figure S46. Emission lifetime decay trace of **L3bc** (λ_{ex} = 372 nm, $\lambda_{detection}$ = 540 nm) in CH_2Cl_2. Fitted with a monoexponential equation CHISQ = 1.024; Durbin-Watson parameter = 2.019

6.7 Low Temperature Emission Studies **Ru1-3**

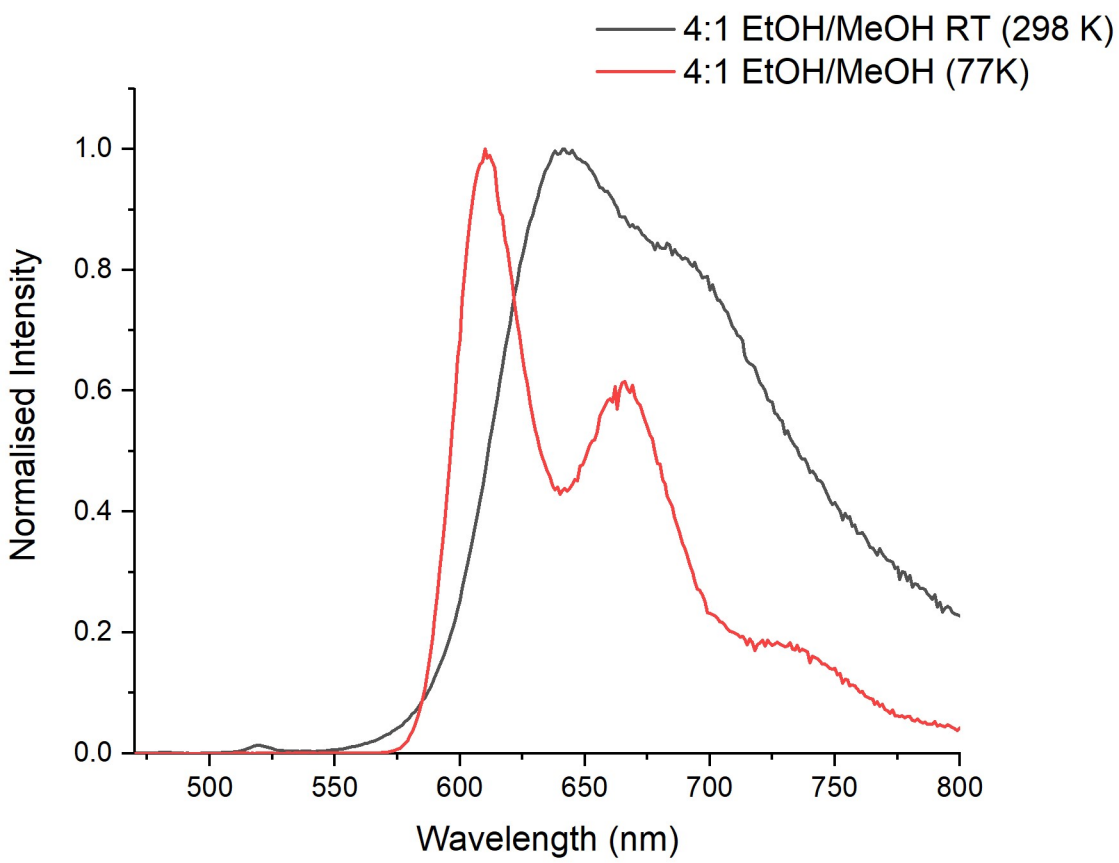

Figure S47. Emission spectra of **Ru1** (λ_{ex} = 450 nm) at 298 K (black line) and 77 k (red line) in 4:1 EtOH:MeOH, 10^{-5} M

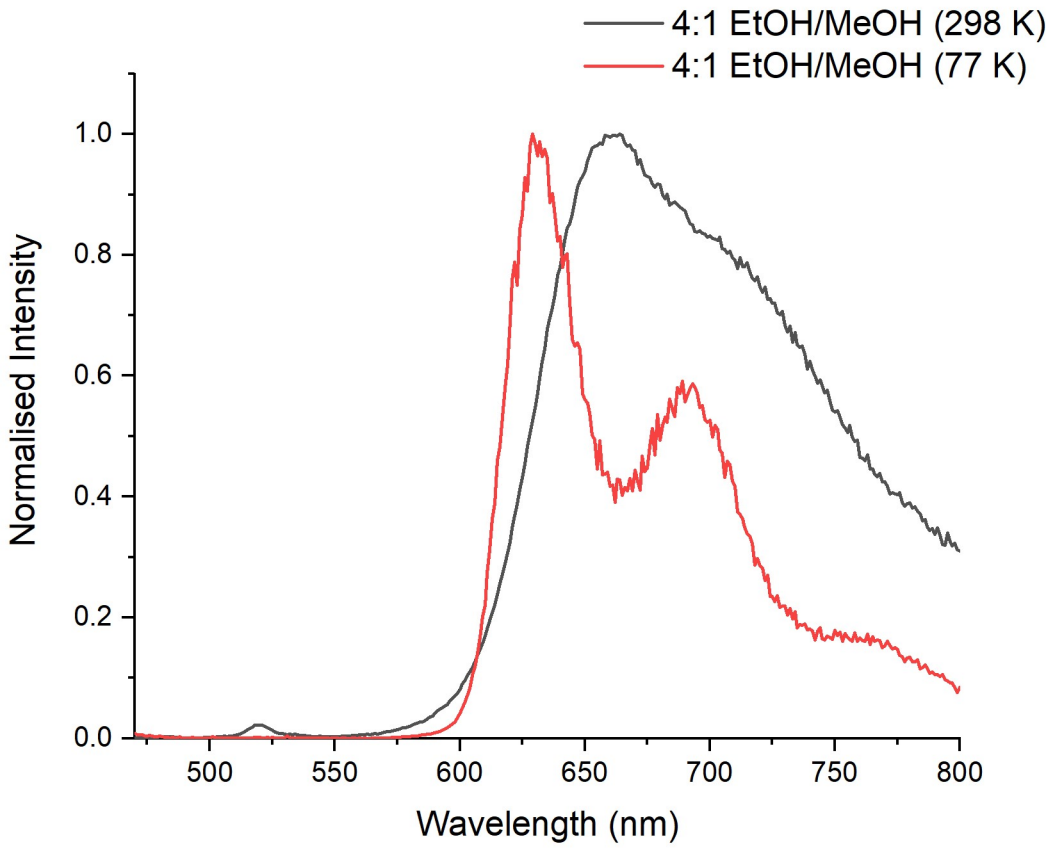

Figure S48. Emission spectra of **Ru2** (λ_{ex} = 450 nm) at 298 K (black line) and 77 k (red line) in 4:1 EtOH:MeOH, 10^{-5} M

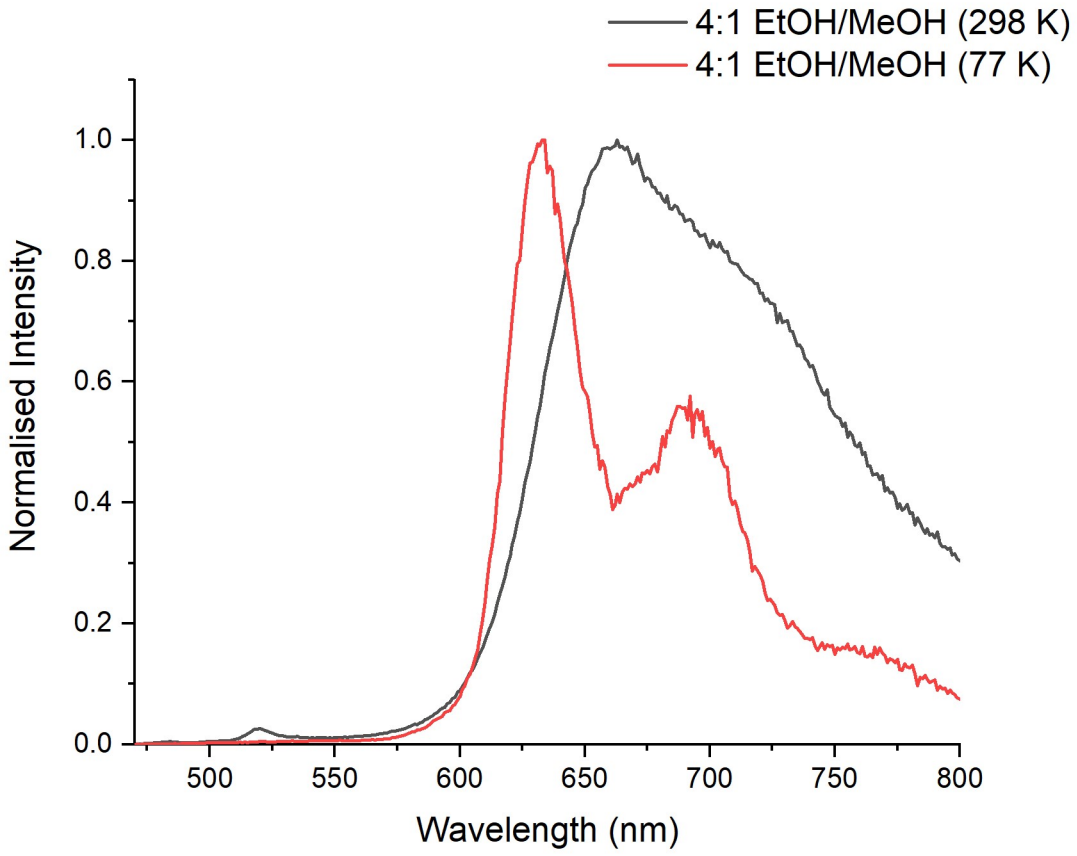

Figure **S49**. Emission spectra of **Ru3** (λex = 450 nm) at 298 K (black line) and 77 k (red line) in 4:1 EtOH:MeOH, 10^{-5} M

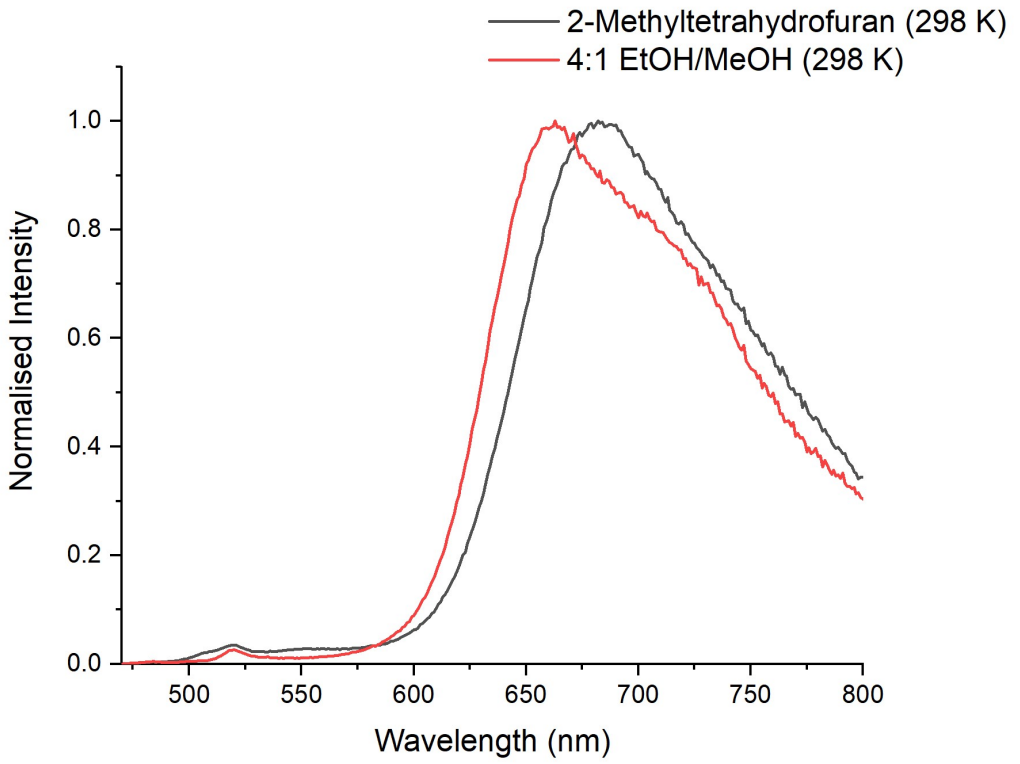

Figure S50. Emission spectra of **Ru3** (λ_{ex} = 450 nm) in 4:1 EtOH:MeOH (red line) and in 2-methyltetrahydrofuran (black line). 298 K, 10^{-5} M

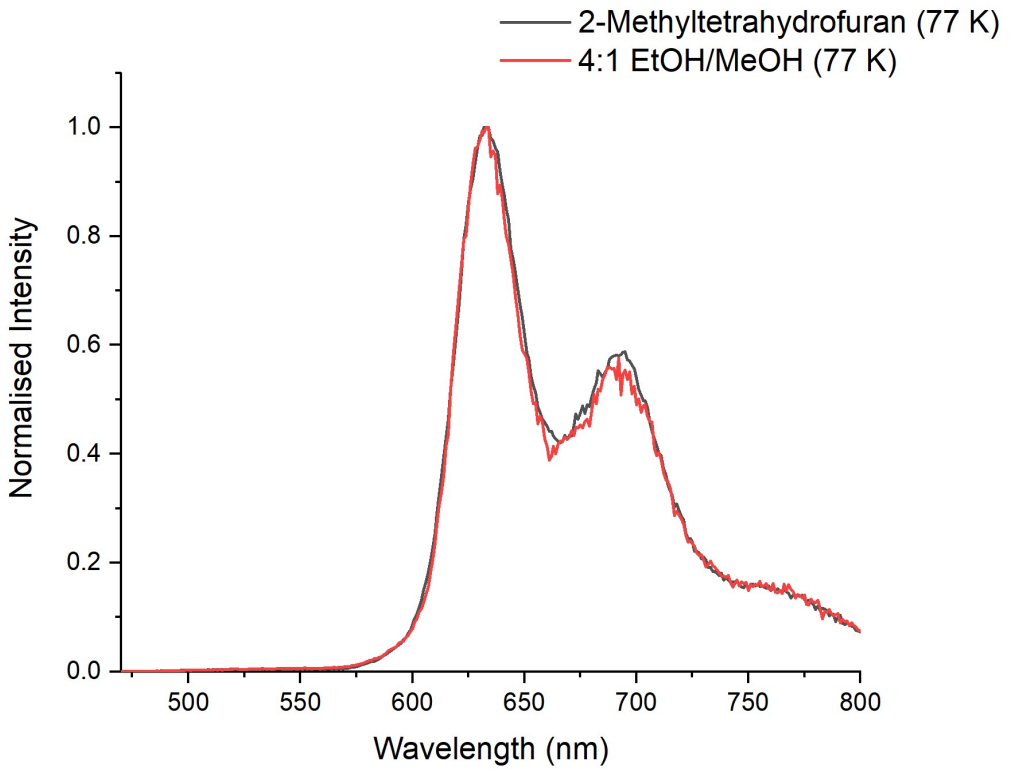

Figure S51. Emission spectra of **Ru1** (λ_{ex} = 450 nm) in 4:1 EtOH:MeOH (red line) and in 2-methyltetrahydrofuran (black line). 77 K, 10^{-5} M

Figure S52. Simplified schematic representation of the emission regimes adopted by **Ru1-3** in CH_2Cl_2 (left) and MeCN (right). In CH_2Cl_2, the emissive excited state has greater ligand character, resulting in longer emission wavelengths, extended emission lifetime and increased quantum yields of phosphorescence. In MeCN, the excited state has greater metal character, resulting in decreased emission wavelength, emission lifetime and quantum yield of phosphorescence.

7.0 References

1 C. Condon, R. Conway-Kenny, X. Cui, L. J. Hallen, B. Twamley, J. Zhao, G. W. Watson and S. M. Draper, *J. Mater. Chem. C*, 2021, **9**, 14573–14577.

2 Z. C. Yang, M. Wang, A. M. Yong, S. Y. Wong, X. H. Zhang, H. Tan, A. Y. Chang, X. Li and J. Wang, *Chem. Commun.*, 2011, **47**, 11615–11617.

3 C. Wu, B. Wang, Y. Wang, J. Hu, J. Jiang, D. Ma and Q. Wang, *J. Mater. Chem. C*, 2019, **7**, 558–566.

4 J. Nociarová, P. Osuský, E. Rakovský, D. Georgiou, I. Polyzos, M. Fakis and P. Hrobárik, *Org. Lett.*, 2021, **23**, 3460–3465.

5 A. M. Horan, V. K. Duong and E. M. McGarrigle, *Org. Lett.*, 2021, **23**, 9089–9093.

6 Bruker (2017). APEX3 v2017.3-0, Bruker AXS Inc., Madison, WI, USA.

7 SADABS: Krause, L., Herbst-Irmer, R., Sheldrick, G. M., Stalke, D. (2015). J. Appl. Cryst. 48, 3-10.

8 Sheldrick, G. M. (2015). Acta Cryst. A71, 3-8

9 Sheldrick, G. M. (2015). Acta Cryst. C71, 3-8.

10 Dolomanov, O.V., Bourhis, L.J., Gildea, R.J, Howard, J.A.K. & Puschmann, H. (2009), J. Appl. Cryst. 42, 339-341.